

A Theoretical and Computational Framework for Isometry Invariant Recognition of Point Cloud Data

Facundo Mémoli¹ and Guillermo Sapiro²

¹Electrical and Computer Engineering
University of Minnesota
Minneapolis, MN 55455, USA
and
Instituto de Ingeniería Eléctrica
Universidad de la República
Montevideo, Uruguay
memoli@ece.umn.edu

²Electrical and Computer Engineering and Digital Technology Center
University of Minnesota
Minneapolis, MN 55455, USA
guille@ece.umn.edu

Abstract. Point clouds are one of the most primitive and fundamental manifold representations. Popular sources of point clouds are three-dimensional shape acquisition devices such as laser range scanners. Another important field where point clouds are found is in the representation of high-dimensional manifolds by samples. With the increasing popularity and very broad applications of this source of data, it is natural and important to work directly with this representation, without having to go through the intermediate and sometimes impossible and distorting steps of surface reconstruction. A geometric framework for comparing manifolds given by point clouds is presented in this paper. The underlying theory is based on Gromov-Hausdorff distances, leading to isometry invariant and completely geometric comparisons. This theory is embedded in a probabilistic setting as derived from random sampling of manifolds, and then combined with results on matrices of pairwise geodesic dis-

Date received: June 24, 2004. Final version received: February 25, 2005. Date accepted: March 9, 2005. Communicated by Peter J. Olver. Online publication: June 30, 2005.

AMS classification: 53C23, 54E35, 60D05, 62P30, 68T10.

Key words and phrases: Point clouds, Gromov-Hausdorff distance, Shape comparison, High-dimensional data, Manifolds, Isometrics.

tances to lead to a computational implementation of the framework. The theoretical and computational results presented here are complemented with experiments for real three-dimensional shapes.

Notation

Symbol	Meaning
\mathbb{R}	Real numbers.
\mathbb{R}^d	d -dimensional Euclidean space
\mathbb{Z}	Integers.
\mathbb{N}	Natural numbers.
(X, d_X)	Metric space X with metric d_X .
X, Y, Z	Metric spaces with metrics d_X, d_Y , and d_Z , respectively.
$B_X(x, r)$	An open ball in the space X , centered at x and with radius r , page 319.
$B_X(\mathbb{X}, r)$	Union of open balls with radius r in the space X , centered at all $x \in \mathbb{X}$, page 319.
\mathbb{X}	Finite subset of the metric space X .
\mathbb{X}_m	Finite subset of the metric space X , with cardinality m .
\mathcal{P}_n	Finite subset of points (Point Cloud) sampled from metric space (cardinality n).
$N_{X,n}^{(R,s)}$	Covering net of X , with n elements, separation s , and covering radius R , page 324.
r_m	Denotes an $r > 0$ such that $X = B_X(\mathbb{X}_m, r)$.
$d_{\mathcal{H}}^Z$	Hausdorff distance between subsets of the metric space Z , page 318.
$d_{\mathcal{GH}}$	Gromov–Hausdorff distance between metric spaces, page 318.
$d_{\mathcal{H}}^{Z, \text{rigid}}$	Rigid isometries' invariant Hausdorff distance between subsets of Z , page 318.
$\text{diam}(X)$	Diameter of the metric space X , page 320.
Π_n	All $n!$ permutations of elements of the set $\{1, \dots, n\}$.
$d_{\mathcal{I}}$	Permutation distance between discrete metric spaces, page 323.
$\mathcal{V}(\mathbb{Z})$	Voronoi partition of Z induced by the points in \mathbb{Z} , page 326.
V_i	Voronoi cell corresponding to the i th point, page 326.
d_B^Z	Bottleneck distance between finite subsets of Z , page 326.
$P_{\vec{p}}(n, m)$	Probability of gathering all n coupons after m trials with probabilities \vec{p} , page 327.
$E_{\vec{p}}(n)$	Expected value of the number of coupons to buy in order to gather all n types, page 327.
I_n	A set of n different indices, $\{i_1, \dots, i_n\}$, page 331.
$\mathbb{X}_m[I_n]$	If $\mathbb{X}_m = \{x_1, \dots, x_m\}$, then it equals the set of points $\{x_{i_1}, \dots, x_{i_n}\}$, page 331.
$d_{\mathcal{F}}$	A partial measure of metric matching, page 17.
Δ_X	A quantity that equals $d_{\mathcal{H}}^X(\mathbb{X}_m, \mathbb{X}_m[I_n])$, page 332.
\mathcal{L}	A quantity which approximates $d_{\mathcal{GH}}(\cdot, \cdot)$. It equals $d_{\mathcal{F}} + \min(\Delta_X, \Delta_Y)$, page 332.

$\mathbf{P}(\mathcal{E})$	Probability of the event \mathcal{E} .
$\mathbf{E}(x)$	Expected value of the random variable x .
h_n	For $n \in \mathbb{N}$, it denotes $\sum_{i=1}^n i^{-1}$, page 327.
\mathcal{S}	Smooth sub-manifold of \mathbb{R}^d .
$\mathbf{a}(\cdot)$	Area measure (on a smooth manifold).
$f_{\mathcal{S}}(r)$	A function equal to $\min_{\{x \in \mathcal{S}\}} \mathbf{a}(B_{\mathcal{S}}(x, r))$, for $r \geq 0$, page 333.
$F_{K,k}(r)$	Equal to $\mathbf{a}(B(\cdot, r))$ on the k -dimensional space of constant curvature K , page 333.

1. Introduction

Point clouds are one of the most primitive and fundamental manifold representations. One of the most popular source of point clouds are three-dimensional shape³ acquisition devices, such as laser range scanners, with applications in geoscience, art (e.g., archival), medicine (e.g., prosthetics), manufacturing (from cars to clothes), and security (e.g., face recognition), among other disciplines. These scanners in general provide raw data in the form of (maybe noisy) unorganized point clouds representing surface samples. With the increasing popularity and very broad applications of this source of data, it is natural and important to work directly with this representation, without having to go to the intermediate step of fitting a surface to it (a step that can add computational complexity and introduce errors). See, e.g., [5], [15], [18], [21], [27], [39], [40], [48], [49] for a few of the recent works with this type of data. Point clouds can also be used as primitives for visualization, e.g., [7], [27], [52], as well as for editing [57].

Another important field where point clouds are found is in the representation of high-dimensional manifolds by samples (see, e.g., [2], [32], [37], [38], [54]). This type of high-dimensional and general codimension data appears in almost all disciplines, from computational biology, to image analysis, to financial data. Due to the extremely high dimensionality in this case, it is impossible to perform manifold reconstruction, and the tasks need to be performed directly on the raw data, meaning the point cloud.

The importance of this type of shape representation is leading to an increase in the fundamental study of point clouds, from its basic geometric characteristics such as curvature [43] and intrinsic distances and geodesics [42], to intrinsic dimensionality and topological structure [2], [13], [16], [17], [22], [54], and also including the detection of particular structures [1] (see also the papers mentioned in the first paragraph and references therein). The goal of this work, inspired in part by [19] and the tools developed in [42], [54], is to develop a theoretical and computational framework to compare shapes represented as point clouds. We are then going to assume the existence of an underlying structure from which our point cloud data

³ We will loosely use the terms shape/object/surface in this Introduction to refer to either surfaces in Euclidean space or to Riemannian manifolds in more generality. A more precise notion will be given later.

are obtained through a sampling/acquisition process. Also, eventually, we introduce the further assumption that the underlying structures we want to comment on all belong to a family or class of objects which satisfy certain tameness properties.

As we have mentioned, a variety of objects can be represented as point clouds in \mathbb{R}^d . One is often presented with the problem of deciding whether two of these point clouds, and/or the corresponding underlying objects or manifolds, represent the same geometric structure or not (*object recognition and classification*). We are then concerned with questions about the underlying unknown structures (objects) which need to be answered, based on discrete measures taken between their respective point clouds. In greater generality, we may wonder what structural information we can gather about the object itself by exploring a point cloud which represents it.⁴

Multidimensional scaling (MDS),⁵ for example, has been used to partly approach this general problem of object analysis/recognition, by means of checking whether the underlying space (object) is flat or not, and also providing information about the object's dimensionality (as a subset of \mathbb{R}^d) and its projection into a reduced space. Procedures based on MDS require that one first computes the interpoint distance matrix for all the members of the point cloud (or for a representative selected subset of them). If one is interested in comparing two different objects, the problem is reduced to a comparison between the corresponding interpoint distance matrices of their point clouds. If the distance we use is the Euclidean one, these matrices only provide information about their *rigid similarity*, and (assuming the matrices are of the same size) if they are equal (up to a permutation of the indices of all elements),⁶ we can only conclude that there exists a rigid isometry (rotation, reflection, translation) from one point cloud to the other. Under assumptions of compactness we can also say something about the true underlying objects. Being more precise, let the point clouds $\mathcal{P}_i \subset S_i$ be ε_i -coverings of the compact surfaces S_i in \mathbb{R}^3 for $i = 1, 2$ (this will be formally defined below). Then assuming there exists a rigid isometry $\tau : \mathbb{R}^3 \rightarrow \mathbb{R}^3$ such that $\tau(\mathcal{P}_1) = \mathcal{P}_2$, we can bound the Hausdorff distance (which we will also formally define below) between $\tau(S_1)$ and S_2 as follows:

$$\begin{aligned} d_{\mathcal{H}}^{\mathbb{R}^3}(\tau(S_1), S_2) &\leq d_{\mathcal{H}}^{\mathbb{R}^3}(\tau(S_1), \tau(\mathcal{P}_1)) + d_{\mathcal{H}}^{\mathbb{R}^3}(\tau(\mathcal{P}_1), \mathcal{P}_2) + d_{\mathcal{H}}^{\mathbb{R}^3}(\mathcal{P}_2, S_2) \\ &= d_{\mathcal{H}}^{\mathbb{R}^3}(S_1, \mathcal{P}_1) + d_{\mathcal{H}}^{\mathbb{R}^3}(\tau(\mathcal{P}_1), \mathcal{P}_2) + d_{\mathcal{H}}^{\mathbb{R}^3}(\mathcal{P}_2, S_2) \\ &\leq \varepsilon_1 + 0 + \varepsilon_2, \end{aligned} \tag{1}$$

⁴ A related important question is: What conditions must a point cloud verify in order to faithfully represent an object, not to mention that one must ascribe a meaning to the word *faithfully*.

⁵ For multidimensional scaling, see, e.g., [6].

⁶ Boutin and Kemper [8], have approached the recognition problem for discrete objects by looking only at the histogram of interpoint squared Euclidean distances. Interestingly, they showed that while there are counterexamples for the recognition problem with this kind of input, they constitute a very small fraction of all the possible point configurations. Such histograms have been used earlier by the Princeton Shape Analysis Group, see www.cs.princeton.edu/gfx/proj/shape/index.html.

and, of course, the same kind of bound holds for the Hausdorff distance between the point clouds once we assume the underlying continuous objects are rigidly isometric, see Section 2.1 below.

One possible modification would be to consider, again for compact surfaces, the *intrinsic* distance instead of the Euclidean (extrinsic) distance for the construction of the aforementioned interpoint distance matrices. A comparison of these new distance matrices would then allow for more freedom in deciding when two objects are similar since now bends are allowed.

If S_1 and S_2 happen to be isometric (here also allowing for bends and not only rigid transformations) we wonder whether we will be able to detect this by looking at (finite) point clouds \mathcal{P}_i sampled from each S_i . This problem is harder to tackle. We approach it through a probabilistic model since, in principle, there might exist, even for the same object, two different samplings that look quite dissimilar (under discrete measures we can cope with computationally) for arbitrarily fine scales (see below).

With the help of the theory presented here we recast these considerations in a rigorous framework and address the case where the distances considered to characterize each point cloud (object) are more general. We concentrate on the case when there exists an intrinsic notion of distance for each object we sample. For the applications of isometry invariant shape (surfaces) recognition, one must therefore consider the distance as measured by paths constrained to travel on the surface of the objects, better referred to as *geodesic distance*.

These ideas have been introduced and used in [9], [19] for bending invariant recognition in three dimensions (without the theoretical foundations introduced here), see also [29]; and also used in [22], [54] to detect intrinsic surface dimensionality. The works [9], [19] argue in favor of invariance to full isometries in the case of face recognition.

In this paper we introduce both a theoretical and computational framework for the so-called *isometry invariant shape recognition problem*. The theory we use, and build our framework upon, is that pioneered by Gromov [25], in which a metric is introduced in the space of all (compact) metric spaces. For the sake of generality we present most of the framework for metric spaces, but the reader, at any moment, is invited to think of surfaces for simplicity. Since we are dealing with both metric spaces and finite sets of samples from them, we are going to speak of continuous and discrete metric spaces. For instance, given a metric space (X, d_X) we consider a finite subset of it, $\mathbb{X}_m \subset X$, which we endow with the metric of X to conform a *discrete* metric space, then X will be called *continuous* (we will use this nomenclature from now on). This is in analogy with the sampling of signals.

The fundamental approach used for isometry invariant recognition in this paper is derived then from the *Gromov–Hausdorff distance*, which we now proceed to present. Suppose X and Y are two (objects) compact subsets of a common larger metric space (Z, d_Z) , and we want to compare X with Y in order to decide whether they are/represent the same object or not. Then, an idea that one might come up with

very early on is that of computing the *Hausdorff distance* between them (see, e.g., [14], [30] for an extensive use of this for shape statistics and image comparison):

$$d_{\mathcal{H}}^Z(X, Y) := \max \left(\sup_{x \in X} d_Z(x, Y), \sup_{y \in Y} d_Z(y, X) \right). \quad (2)$$

But what happens if we want to allow for certain deformations to occur and still decide that the objects are the same? More precisely, we are interested in being able to find a distance between metric spaces that is *blind* to isometric transformations (“bends”). This will permit a truly geometric comparison between the manifolds, independent of their embedding and bending position. Following [25], we introduce the *Gromov–Hausdorff distance* between metric spaces:

$$d_{\mathcal{GH}}(X, Y) := \inf_{Z, f, g} d_{\mathcal{H}}^Z(f(X), g(Y)), \quad (3)$$

where $f : X \rightarrow Z$ and $g : Y \rightarrow Z$ are *isometric embeddings* (distance preserving) into the metric space Z . It turns out that this measure of metric proximity between metric spaces is well suited for our problem and will allow us to give a formal framework to address the isometric shape recognition problem (for point cloud data). However, this notion of distance between metric spaces encodes the “metric” disparity between them, at first glance, in a computationally impractical way. We derive below new results that connect this notion of disparity with other more computationally appealing expressions.

Remark 1. In [19] it was proposed to use MDS applied to the geodesic distance matrices of each point cloud in order to obtain a new pair of point clouds in \mathbb{R}^3 , such that the Euclidean distance matrices of these new point clouds resemble as closely as possible (according to some criterion) the geodesic distance matrices between the original point clouds. The comparison then proceeds by computing some metric in \mathbb{R}^3 to measure the dissimilarity between the new point clouds. One could use, for example, the rigid-isometries invariant Hausdorff distance $d_{\mathcal{H}}^{\mathbb{R}^3, \text{rigid}}(\cdot, \cdot)$, see Section 2.1 below. This process can be rewritten in a more appealing way as follows. Let $\mathcal{P}_1 \subset \mathbb{R}^3$ and $\mathcal{P}_2 \subset \mathbb{R}^3$ be the original point clouds and let $\mathcal{Q}_1 \subset \mathbb{R}^3$ and $\mathcal{Q}_2 \subset \mathbb{R}^3$ be the corresponding new (projected) point clouds. Also let $\hat{f} : \mathbb{R}^3 \rightarrow \mathbb{R}^3$ and $\hat{g} : \mathbb{R}^3 \rightarrow \mathbb{R}^3$ be such that $\hat{f}(\mathcal{P}_1) = \mathcal{Q}_1$ and $\hat{g}(\mathcal{P}_2) = \mathcal{Q}_2$. Then, the number we compute is $d_{\mathcal{H}}^{\mathbb{R}^3, \text{rigid}}(\hat{f}(\mathcal{P}_1), \hat{g}(\mathcal{P}_2))$ which has an interesting resemblance with the formula in the definition of the Gromov–Hausdorff distance.⁷

Since we have in mind specific applications and scenarios such as those described above, and in particular surfaces and submanifolds of some Euclidean space \mathbb{R}^d , we assume that we are given as input points *densely* sampled from the

⁷ Of course, \hat{f} and \hat{g} are not isometries, in general.

metric spaces (surfaces, manifolds). This will manifest itself in many places in the theory described below. We will present a way of computing a discrete approximation (or bound) to $d_{\mathcal{GH}}(\cdot, \cdot)$ based on the metric information provided by these point clouds.

Our problem of isometry invariant shape recognition can be split in two parts. First, suppose the metric spaces under consideration happen to be isometric. We then have to guarantee that we can discover this by looking at a computable discrete measure of metric similarity based just on our observed data, that is, the point clouds. Second, if that measure of (discrete) metric similarity is “small,” what can we say about that metric similarity between the underlying metric spaces? Both parts are addressed in this paper. One cannot perform object recognition without either of them.

The rest of this paper is organized as follows. The basic theoretical foundations are given in Section 2, Section 3 presents the computational foundations, Section 4 illustrates the use of the framework with real examples and, finally, Section 5 concludes the paper and describes current efforts and future directions.

We should note that this is a mainly theoretical paper which proposes a framework (that leads to a possible practical algorithm) and that the examples provided in Section 4 are not exhaustive and do not make use of all the machinery introduced here, they simply exemplify and illustrate the application of the framework. More comprehensive experimentation is the subject of current efforts and will be reported in subsequent publications.

2. Theoretical Foundations

This section covers the fundamental theory behind the bending invariant recognition framework we develop. We first introduce some basic notation, definitions, and classical results. We use basic concepts on metric spaces, see, e.g., [33] for a simple exposition of this.

Definition 1 (Metric Space). A set M is a metric space if for every pair of points $x, y \in M$ there is a well-defined function $d_M(x, y)$ whose values are nonnegative real numbers, such that:

- (a) $d_M(x, y) = 0$ if and only if $x = y$; and
- (b) $d_M(x, y) \leq d_M(y, z) + d_M(z, x)$ for any x, y , and $z \in M$.

We call $d_M : M \times M \rightarrow \mathbb{R}$ the metric or distance. For clarity we will specify a metric space as the pair (M, d_M) .

Definition 2 (Covering). For a point x in the metric space (X, d_X) and $r > 0$, we will denote by $B_X(x, r)$ the set $\{z \in X \mid d_X(x, z) < r\}$. For a subset A of X , we use the notation $B_X(A, r) = \cup_{a \in A} B_X(a, r)$. We say that a set $C \subset X$ is an R -covering of X if $B_X(C, R) = X$. We will also frequently say that the set A is

an n -covering of X if A constitutes, for some $r > 0$, a covering of X by n -balls with centers in points of A .

Definition 3 (Isometry). We say the metric spaces (X, d_X) and (Y, d_Y) are isometric when there exists a bijective mapping $\Phi : X \rightarrow Y$ such that $d_X(x_1, x_2) = d_Y(\Phi(x_1), \Phi(x_2))$ for all $x_1, x_2 \in X$. Such a Φ is an isometry between (X, d_X) and (Y, d_Y) .

Next, we state some well-known properties of the Gromov–Hausdorff distance $d_{\mathcal{GH}}(\cdot, \cdot)$ which will be useful for our presentation.

Proposition 1.

1. Let (X, d_X) , (Y, d_Y) , and (Z, d_Z) be metric spaces, then

$$d_{\mathcal{GH}}(X, Y) \leq d_{\mathcal{GH}}(X, Z) + d_{\mathcal{GH}}(Z, Y).$$

2. If $d_{\mathcal{GH}}(X, Y) = 0$ and (X, d_X) , (Y, d_Y) are compact metric spaces, then (X, d_X) and (Y, d_Y) are isometric.
3. Let $\{x_1, \dots, x_n\} \subset X$ be an R -covering of the compact metric space (X, d_X) . Then $d_{\mathcal{GH}}(X, \{x_1, \dots, x_n\}) \leq R$.
4. For compact metric spaces (X, d_X) and (Y, d_Y) ,

$$\frac{1}{2} |\mathbf{diam}(X) - \mathbf{diam}(Y)| \leq d_{\mathcal{GH}}(X, Y) \leq \frac{1}{2} \max(\mathbf{diam}(X), \mathbf{diam}(Y)),$$

where $\mathbf{diam}(X) := \max_{x, x' \in X} d_X(x, x')$ stands for the diameter of the metric space (X, d_X) .

5. For bounded metric spaces (X, d_X) and (Y, d_Y) ,

$$d_{\mathcal{GH}}(X, Y) = \inf_{\substack{\varphi : X \rightarrow Y \\ \psi : Y \rightarrow X}} \sup_{\substack{x_1, x_2 \in X \\ y_1, y_2 \in Y \\ (x_i, y_i) \in \mathcal{G}(\varphi, \psi)}} \frac{1}{2} |d_X(x_1, x_2) - d_Y(y_1, y_2)|,$$

where $\mathcal{G}(\varphi, \psi) = \{(x, \varphi(x)), x \in X\} \cup \{(\psi(y), y), y \in Y\}$ and the infimum is taken over all arbitrary maps $\varphi : X \rightarrow Y$ and $\psi : Y \rightarrow X$.

The proofs of Properties 1 to 4 of Proposition 1 can be gleaned from [10], [25], [28], [50], and Property 5 can be found in [34]. Also of great informative value is [51].

Remark 2. Note that Property 5 in Proposition 1 can be recast in a somewhat clearer form: Let

$$\begin{aligned} A(\varphi) &= \sup_{x_1, x_2 \in X} |d_X(x_1, x_2) - d_Y(\varphi(x_1), \varphi(x_2))|, \\ B(\psi) &= \sup_{y_1, y_2 \in Y} |d_X(\psi(y_1), \psi(y_2)) - d_Y(y_1, y_2)|, \\ \text{and } C(\varphi, \psi) &= \sup_{x \in X, y \in Y} |d_X(x, \psi(y)) - d_Y(\varphi(x), y)|, \end{aligned}$$

then

$$d_{\mathcal{GH}}(X, Y) = \inf_{\substack{\varphi : X \rightarrow Y \\ \psi : Y \rightarrow X}} \frac{1}{2} \max (A(\varphi), B(\psi), C(\varphi, \psi)). \quad (4)$$

It is interesting to note the following: Assume that $d_{\mathcal{GH}}(X, Y) \leq \eta$ for small η , then, roughly speaking, we can find φ and ψ such that:

- (1) φ provides a low metric distortion map from X to Y (because $A(\varphi) \leq 2\eta$);
- (2) ψ provides a low metric distortion map from Y to X (because $B(\psi) \leq 2\eta$); and
- (3) φ and ψ are “almost” inverses of one another (because $C(\varphi, \psi) \leq 2\eta$; then taking $y = \varphi(x)$ in the definition of C we find $d_X(x, \psi(\varphi(x))) \leq 2\eta$ for all $x \in X$; and also, symmetrically, $d_Y(y, \varphi(\psi(y))) \leq 2\eta$ for all $y \in Y$).

Remark 3. From Property 4 in Proposition 1 it follows that two metric spaces whose diameters differ must be at a positive $d_{\mathcal{GH}}(\cdot, \cdot)$ distance, as intuition requires.

From Properties 1–5 of Proposition 1, we can also easily obtain the following important result:

Corollary 1. *Let X and Y be compact metric spaces. Let, moreover, \mathbb{X}_m be an r -covering of X (consisting of m points) and let $\mathbb{Y}_{m'}$ be an r' -covering of Y (consisting of m' points). Then*

$$|d_{\mathcal{GH}}(X, Y) - d_{\mathcal{GH}}(\mathbb{X}_m, \mathbb{Y}_{m'})| \leq r + r'.$$

We can then say that if we could compute $d_{\mathcal{GH}}(\cdot, \cdot)$ for discrete metric spaces, which are dense enough samplings of the “continuous” underlying ones, that number would be a good approximation to what happens between the continuous spaces. Currently, there is no computationally efficient way to directly compute $d_{\mathcal{GH}}(\cdot, \cdot)$ between discrete metric spaces in general. This forces us to develop a roundabout path, see Section 2.2 below. Before going into the general case, we discuss next the application of the ideas of our framework to a simpler but important case.

2.1. Intermezzo: The Case of Rigid Isometries

When we try to compare two (compact) subsets X and Y of a larger metric space Z , the situation is a bit simpler. The measure of similarity boils down to a somewhat simpler Hausdorff distance between the sets (which, of course, must take into account self-isometries of Z). In more detail, one must compute

$$d_{\mathcal{H}}^{Z, \text{rigid}}(X, Y) := \inf_{\Phi} d_{\mathcal{H}}^Z(X, \Phi(Y)), \quad (5)$$

where $\Phi : Z \rightarrow Z$ ranges over all self-isometries of Z . If we knew an efficient

way of computing $\inf_{\Phi} d_{\mathcal{H}}^Z(X, \Phi(Y))$, then this restricted shape recognition problem would be well posed for Z , in view of an adapted version of Proposition 1 and Corollary 1, as soon as we can give guarantees of coverage. For the sake of completeness we state such a result.

Proposition 2. $d_{\mathcal{H}}^{Z, \text{rigid}}(\cdot, \cdot)$ satisfies the triangle inequality and, in particular, the following relation holds:

$$|d_{\mathcal{H}}^{Z, \text{rigid}}(X, Y) - d_{\mathcal{H}}^{Z, \text{rigid}}(\mathbb{X}_m, \mathbb{Y}_{m'})| \leq r + r'$$

for compact $X, Y \subset Z$ such that $X \subset B_Z(\mathbb{X}_m, r)$ and $Y \subset B_Z(\mathbb{Y}_{m'}, r')$.

Coverage can be guaranteed, in the case of submanifolds of \mathbb{R}^d , by imposing a probabilistic model on the samplings \mathbb{X}_m of the manifolds, and a bound on the curvatures of the family of manifolds one wishes to work with. In more detail, for given $r > 0$ and $p \in (0, 1)$, we can show that there exists finite $m_{p,r}$ such that

$$\mathbf{P}(d_{\mathcal{H}}^{\mathbb{R}^d}(X, \mathbb{X}_m) > r) \leq 1 - p$$

for $m \geq m_{p,r}$, see Section 3.2.

In the case of surfaces in $Z = \mathbb{R}^3$, Φ sweeps all rigid isometries, and there exist good algorithms which can actually solve the problem approximately. For example, in [23] the authors report an algorithm which, for any given $0 < \alpha < 1$, can find a rigid transformation $\widehat{\Phi}_{\alpha}$ such that

$$d_{\mathcal{H}}^{\mathbb{R}^3}(\mathbb{X}_m, \widehat{\Phi}_{\alpha}(\mathbb{Y}_{m'})) \leq (8 + \alpha) \inf_{\Phi} d_{\mathcal{H}}^{\mathbb{R}^3}(\mathbb{X}_m, \Phi(\mathbb{Y}_{m'}))$$

with complexity $O(s^4 \log s)$ where $s = \max(m, m')$. This computational result, together with simple considerations, makes the problem of surface recognition (under rigid motions) well posed and well justified. In fact, using Proposition 2 we obtain a bound between the distance we want to estimate $d_{\mathcal{H}}^{\mathbb{R}^3, \text{rigid}}(X, Y)$ and the observable (computable) value $d_{\mathcal{H}}^{\mathbb{R}^3}(\mathbb{X}_m, \widehat{\Phi}_{\alpha}(\mathbb{Y}_{m'}))$:

$$\begin{aligned} d_{\mathcal{H}}^{\mathbb{R}^3, \text{rigid}}(X, Y) - (r + r') &\leq d_{\mathcal{H}}^{\mathbb{R}^3}(\mathbb{X}_m, \widehat{\Phi}_{\alpha}(\mathbb{Y}_{m'})) \\ &\leq 10 (d_{\mathcal{H}}^{\mathbb{R}^3, \text{rigid}}(X, Y) + (r + r')). \end{aligned} \quad (6)$$

Equation (6) gives a formal justification to the procedure outlined for this surface recognition problem. To the best of our knowledge, this is the first time such formality is presented for this very important problem, both in the particular case just shown and for the general case addressed next. In any case, if d_S is the measure of similarity we are considering, and $\widehat{d_S}$ is the *computable* approximate measure of similarity, the kind of relation we seek to establish is

$$A(d_S(X, Y) - \alpha) \leq \widehat{d_S}(\mathbb{X}_m, \mathbb{Y}_{m'}) \leq B(d_S(X, Y) + \beta) \quad (7)$$

for some constants A, B and numbers α and β which can be made small by refining the samplings. Moreover, it may happen that relation (7) holds *with a*

certain probability. Every recognition task needs to be supported by a relation of this type, see also [45].

2.2. The General Case

The theory introduced by Gromov addresses the concept of metric approximation between metric spaces. When dealing with discrete metric spaces, such as those arising from samplings or coverings of continuous ones, it is convenient to introduce another distance between them which ultimately is the one we compute for point clouds, see Section 3.6 below. For discrete metric spaces (both of cardinality n) ($\mathbb{X} = \{x_1, \dots, x_n\}, d_{\mathbb{X}}$) and ($\mathbb{Y} = \{y_1, \dots, y_n\}, d_{\mathbb{Y}}$) we define the distance:⁸

$$d_{\mathcal{I}}(\mathbb{X}, \mathbb{Y}) := \min_{\pi \in \Pi_n} \max_{1 \leq i, j \leq n} \frac{1}{2} |d_{\mathbb{X}}(x_i, x_j) - d_{\mathbb{Y}}(y_{\pi_i}, y_{\pi_j})|, \quad (8)$$

where Π_n stands for the set of all permutations of $\{1, \dots, n\}$. A permutation π provides the correspondence between the points in the sets, and $|d_{\mathbb{X}}(x_i, x_j) - d_{\mathbb{Y}}(y_{\pi_i}, y_{\pi_j})|$ gives the pointwise distance/disparity once this correspondence has been assumed.

It is evident that one has, by virtue of Property 5 of Proposition 1 (and Remark 2, if we take the infimum over invertible maps $\psi = \varphi^{-1}$):

$$d_{\mathcal{GH}}(\mathbb{X}, \mathbb{Y}) \leq d_{\mathcal{I}}(\mathbb{X}, \mathbb{Y}). \quad (9)$$

Moreover, we easily derive the following bound, whose usefulness will be made evident in Section 3.

Corollary 2. *Let (X, d_X) and (Y, d_Y) be compact metric spaces. Let $\mathbb{X} = \{x_1, \dots, x_n\} \subset X$ and $\mathbb{Y} = \{y_1, \dots, y_n\} \subset Y$, such that $B_X(\mathbb{X}, R_X) = X$ and $B_Y(\mathbb{Y}, R_Y) = Y$ (the point clouds provide R_X and R_Y coverings, respectively). Then*

$$d_{\mathcal{GH}}(X, Y) \leq R_X + R_Y + d_{\mathcal{I}}(\mathbb{X}, \mathbb{Y}), \quad (10)$$

with the understanding that $d_{\mathbb{X}} = d_X|_{\mathbb{X} \times \mathbb{X}}$ and $d_{\mathbb{Y}} = d_Y|_{\mathbb{Y} \times \mathbb{Y}}$.

Remark 4. This result tells us that if we manage to find coverings of X and Y for which the distance $d_{\mathcal{I}}$ is small, then if the radii of those coverings are also small, the underlying manifolds X and Y sampled by these point clouds must be close in a metric sense. Another way of interpreting this is that we will never see a small value of $d_{\mathcal{I}}(\mathbb{X}, \mathbb{Y})$ whenever $d_{\mathcal{GH}}(X, Y)$ is large, a simple statement with practical value, since we will only be able to look at values of $d_{\mathcal{I}}$, which depend on the point clouds. This is because, in contrast with $d_{\mathcal{GH}}(\cdot, \cdot)$, the distance $d_{\mathcal{I}}$ is (approximately) computable from the point clouds, see Section 3.6.

We now introduce some additional notation regarding coverings of metric spaces. Given a metric space (X, d_X) , the discrete subset $N_{X,n}^{(R,s)}$ denotes a set of

⁸ One can easily check that this is really a distance.

points $\{x_1, \dots, x_n\} \subset X$ such that: (1) $B_X(N_{X,n}^{(R,s)}, R) = X$; and (2) $d_X(x_i, x_j) \geq s$ whenever $i \neq j$. In other words, the set constitutes an R -covering and the points in the set are not too close to each other.

Remark 5. For each $r > 0$ denote by $N(r, X)$ the minimum number of closed balls of radii r needed to cover X . Then [50, Chap. 10] we can actually show that the class $(\mathcal{M}, d_{\mathcal{GH}})$, of all compact metric spaces X whose covering number $N(r, X)$ are bounded for all (small) positive r by a function $N : (0, C_1) \rightarrow (0, \infty)$, is *totally bounded*. This means that given $\rho > 0$, there exist a finite positive integer $k(\rho)$ and compact metric spaces $X_1, \dots, X_{k(\rho)} \in \mathcal{M}$ such that for any $X \in \mathcal{M}$ one can find $i \in \{1, \dots, k(\rho)\}$ such that $d_{\mathcal{GH}}(X, X_i) \leq \rho$. This is very interesting from the point of view of applications since it gives formal justification to the classification problem of metric spaces. For example, in a system of storage/retrieval of faces/information manifolds, this concept permits the design of a clustering procedure for the shapes.

The following proposition will also be fundamental for our computational framework in Section 3.

Proposition 3 ([25]). *Let (X, d_X) and (Y, d_Y) be any pair of given compact metric spaces and let $\eta = d_{\mathcal{GH}}(X, Y)$. Also, let $N_{X,n}^{(R,s)} = \{x_1, \dots, x_n\}$ be given. Then, given $\alpha > 0$ there exist points $\{y_1^\alpha, \dots, y_n^\alpha\} \subset Y$ such that:*

- (1) $d_{\mathcal{I}}(N_{X,n}^{(R,s)}, \{y_1^\alpha, \dots, y_n^\alpha\}) \leq (\eta + \alpha)$;
- (2) $B_Y(\{y_1^\alpha, \dots, y_n^\alpha\}, R + 2(\eta + \alpha)) = Y$; and
- (3) $d_Y(y_i^\alpha, y_j^\alpha) \geq s - 2(\eta + \alpha)$ for $i \neq j$.

Remark 6. Proposition 3 tells us that if the metric spaces happen to be sufficiently close in a metric sense, then given an s -separated covering on one of them, one can find an $(s'$ -separated) covering in the other metric space such that $d_{\mathcal{I}}$ between those coverings (point clouds) is also small. This, in conjunction with Remark 4, proves that in fact our goal of trying to determine the metric similarity of metric spaces based on discrete observations of them is, so far, a (theoretically) well-posed problem.

Since by Tychonoff's theorem the n -fold product space $Y \times \dots \times Y$ is compact, if $s - 2\eta \geq c > 0$ for some positive constant c , by passing to the limit along the subsequences of $\{y_1^\alpha, \dots, y_n^\alpha\}_{\{\alpha > 0\}}$ above (if needed) one can assume the existence of a set of different points $\{\bar{y}_1, \dots, \bar{y}_n\} \subset Y$ such that $d_{\mathcal{I}}(\{\bar{y}_1, \dots, \bar{y}_n\}, N_{X,n}^{(R,s)}) \leq \eta$, $\min_{i \neq j} d_Y(\bar{y}_i, \bar{y}_j) \geq s - 2\eta > 0$, and $B_Y(\{\bar{y}_1, \dots, \bar{y}_n\}, R + 2\eta) = Y$.

Since we are only given finite sets of points sampled from each metric space, the existence of $\{\bar{y}_1, \dots, \bar{y}_n\}$ guaranteed by Proposition 3 and Remark 6 doesn't seem to make our life a lot easier since those points could very well not be contained in our given finite datasets. The simple idea of using a triangle inequality (with metric

$d_{\mathcal{I}}$) to deal with this does not work in principle, since one can find, for the same underlying space, two covering nets whose $d_{\mathcal{I}}$ distance is not small, see [11], [41]. Let us explain this in more detail. Assume that as input we are given two finite sets of points \mathbb{X}_m and \mathbb{Y}_m on two metric spaces, X and Y , respectively, which we assume to be isometric. Then the results above ensure that for any given $N_{X,n}^{(R,s)} \subset \mathbb{X}_m$ there exists an $N_{Y,n}^{(R,s)} \subset Y$ such that $d_{\mathcal{I}}(N_{X,n}^{(R,s)}, N_{Y,n}^{(R,s)}) = 0$. However, it is clear that this $N_{Y,n}^{(R,s)}$ has no reason to be contained in the given point cloud \mathbb{Y}_m . The obvious idea would be to try to rely on some kind of property of independence on the sample representing a given metric space, namely that for any two different covering nets N_1 and N_2 (of the same cardinality and with small covering radii) of X the distance $d_{\mathcal{I}}(N_1, N_2)$ is also small. If this were granted, we could proceed as follows:

$$\begin{aligned} d_{\mathcal{I}}(N_{X,n}^{(R,s)}, N_{Y,n}^{(\hat{R},\hat{s})}) &\leq d_{\mathcal{I}}(N_{X,n}^{(R,s)}, N_{Y,n}^{(R,s)}) + d_{\mathcal{I}}(N_{Y,n}^{(\hat{R},\hat{s})}, N_{Y,n}^{(R,s)}) \\ &= 0 + \text{small}(R, \hat{R}), \end{aligned} \quad (11)$$

where $\text{small}(R, \hat{R})$ is a small number depending only on R and \hat{R} . The property we fancy to rely upon was conjectured by Gromov in [26] (see also [55]) and disproved by Burago and Kleiner in [11] and McMullen in [41], see also [47] for certain positive results. Their counterexamples are for separated covering nets in \mathbb{Z}^2 . It is not known whether one can construct counterexamples for compact metric spaces, or if there exists a characterization of a family of n -points separated covering nets of a given compact metric space such that any two of them are at a small $d_{\mathcal{I}}$ -distance which can be somehow controlled by n . A first step toward this is the density condition introduced in [12].

If counterexamples didn't exist for compact metric spaces, then the above inequality would be sufficient. Without assuming this, we give below an argument which tackles the problem in a probabilistic way. In other words, we use a probabilistic approach to bound $d_{\mathcal{I}}$ for two different samples from a given metric space. For this, we pay the price of assuming the existence of a measure which comes with our metric space.⁹ On the other hand, probabilistic frameworks are natural for (maybe noisy) random samples of manifolds as obtained in real applications.¹⁰

2.3. A Probabilistic Setting for Submanifolds of \mathbb{R}^d

We now limit ourselves to smooth Riemannian submanifolds of \mathbb{R}^d endowed with the metric inherited from ambient space. However, the work can be extended to

⁹ In the present paper we therefore deal only with the case of submanifolds of \mathbb{R}^d .

¹⁰ In more generality, data are acquired by sensors or arrays of sensors which return a value in \mathbb{R}^d for some $d \geq 1$. The acquisition process or the sensors themselves might be subject to some perturbations (miscalibrations of mechanical parts of a three-dimensional scanner, electric noise in electrodes, etc.). Under the assumption of the existence of an underlying structure from which the data are sampled, it therefore seems sensible to introduce a probability measure which models the acquisition process.

more general metric spaces, see further comments in Section 5.2. In what follows, for an *event* \mathcal{E} , $\mathbf{P}(\mathcal{E})$ will denote its probability and for a random variable x , $\mathbf{E}(x)$ will denote its expected value.

Let Z be a smooth and compact submanifold of \mathbb{R}^d with intrinsic (geodesic) distance function $d_Z(\cdot, \cdot)$. We can now speak more freely about points $\{z_i\}_{i=1}^m$ sampled uniformly from X : We say that the random point \widehat{z} is *uniformly distributed* on Z if, for any measurable $C \subset Z$, $\mathbf{P}(\widehat{z} \in C) = \mathbf{a}(C)/\mathbf{a}(Z)$, where $\mathbf{a}(B)$ denotes the area of the measurable set $B \subset Z$. This uniform probability measure can be replaced by other probability measures which, for example, adapt to the geometry of the underlying surface, and the framework here developed can be extended to those as well, see the comments in Section 5.2.

Let $\mathbb{Z} = \{z_1, \dots, z_n\}$ and $\mathbb{Z}' = \{z'_1, \dots, z'_n\}$ be two discrete subsets of Z (two point clouds). For any permutations $\pi \in \Pi_n$ and $i, j \in \{1, \dots, n\}$,

$$|d_Z(z_i, z_j) - d_Z(z'_{\pi_i}, z'_{\pi_j})| \leq d_Z(z_i, z'_{\pi_i}) + d_Z(z_j, z'_{\pi_j})$$

and, therefore, we have

$$d_B^Z(\mathbb{Z}, \mathbb{Z}') := \min_{\pi \in \Pi_n} \max_k d_Z(z_k, z'_{\pi_k}) \geq d_I(\mathbb{Z}, \mathbb{Z}'). \quad (12)$$

This is known as the *bottleneck distance* between \mathbb{Z} and \mathbb{Z}' , both being subsets of Z . This is one possible way of measuring the distance between two different samples of the same metric space.¹¹

Instead of dealing with (11) deterministically, after imposing conditions on the underlying metric spaces X and Y , we derive probabilistic bounds for the left-hand side. We also make evident that, by suitable choices of the relations among the different parameters, this probability can be chosen at will. This result is then used to bound the distance d_I between two point cloud samples of a given metric space, thereby leading to the type of bound expressed in eq. (11) and from this the bounds on the original Gromov–Hausdorff distance between the underlying objects.

We introduce the *Voronoi diagram* $\mathcal{V}(\mathbb{Z})$ on Z , determined by the points in \mathbb{Z} (see, e.g., [36]). The i th Voronoi cell of the Voronoi diagram defined by $\{z_1, \dots, z_n\} \subset Z$ is given by

$$V_i := \left\{ z \in Z \mid d_Z(z_i, z) < \min_{j \neq i} d_Z(z_j, z) \right\}. \quad (13)$$

We then have $Z = \bigsqcup_{k=1}^n \overline{V_k}$.

Lemma 1.

- (1) *If the points $\{z_1, \dots, z_n\}$ are s -separated, then, for any $1 \leq i \leq n$, $B_Z(z_i, s/2) \subset V_i$.*

¹¹ In [47], this distance is used to establish the equivalence (according to this notion) of separated nets in certain hyperbolic metric spaces.

- (2) *If the points $\{z_1, \dots, z_n\}$ constitute an R -covering of Z , then $V_i \subseteq B_Z(z_i, R)$ for all $i = 1, \dots, n$.*

Proof. To prove (1) first note that for any $z \in Z$ and $i \neq j$, $d_Z(z, z_i) + d_Z(z, z_j) \geq s$ by the triangle inequality. Assume in particular that $z \in B_Z(z_i, s/2)$, then $d_Z(z, z_i) < s/2$ and $d_Z(z, z_j) > s/2$ for all $j \neq i$, then $z \in V_i$. To prove (2) assume $z \in V_i$ but $z \notin B_Z(z_i, R)$, that is, $d_Z(z, z_i) \geq R$. But since $\{z_1, \dots, z_n\}$ is an R -covering of Z , z must belong to a certain $B_Z(z_k, R)$ for some $k \neq i$, that is, $d_Z(z, z_k) < R$. But then, z is closer to z_k than to z_i , which contradicts $z \in V_i$. \square

We consider Z to be fixed, and we assume $Z' = \{z'_1, \dots, z'_n\}$ to be chosen from a set $Z_m \subset Z$ consisting of $m \gg n$ i.i.d. points sampled uniformly from Z .

We first want to find, amongst points in Z_m , n different points $\{z_{i_1}, \dots, z_{i_n}\}$ such that each of them belongs to one Voronoi cell, $\{z_{i_k} \in V_k \text{ for } k = 1, \dots, n\}$; we provide lower bounds for $\mathbf{P}(\#(V_k \cap Z_m) \geq 1, \ 1 \leq k \leq n)$, the probability that this happens.

We can see the event as if we *collected* points inside all the Voronoi cells, a case of the *Coupon Collecting Problem*, see [20]. We buy merchandise at a coupons-giving store until we have collected all possible types of coupons. The next lemma presents the basic results we need about this concept. These results are due to Von Schelling [56] and Borwein and Hijab [4].

Lemma 2 (Coupon Collecting). *If there are n different coupons one wishes to collect, such that the probability of seeing the k th coupon is $p_k \in (0, 1)$ (let $\vec{p} = (p_1, \dots, p_n)$), and one obtains samples of all of them in an independent way, then:*

- (1) ([56]). *The probability $P_{\vec{p}}(n, m)$ of having collected all n coupons after m trials is given by*

$$P_{\vec{p}}(n, m) = 1 - S_n \left(\sum_{j=2}^n (-1)^j \left(\sum_{k=j}^n p_k \right)^m \right), \quad (14)$$

where the symbol S_n means that we consider all possible combinations of the n indices in the expression being evaluated.¹²

- (2) ([4]). *The expected value of the number of trials needed to collect all the coupons is given by*

$$E_{\vec{p}}(n) = \mathbf{E} \left(\max_{1 \leq i \leq n} \frac{X_i}{p_i} \right), \quad (15)$$

where X_i are independent positive random variables satisfying $\mathbf{P}(X_i > t) = e^{-t}$ for $t \geq 0$ and $1 \leq i \leq n$.

¹² For example, $S_3((p_1 + p_2)^k) = (p_1 + p_2)^k + (p_1 + p_3)^k + (p_2 + p_3)^k$.

For $n \in \mathbb{N}$, let $h_n := \sum_{i=1}^n i^{-1}$.

Corollary 3. $P_{\vec{p}}(n, m) \geq 1 - h_n/m \cdot \min_k p_k$.

Proof. By Markov's inequality, $1 - P_{\vec{p}}(n, m) \leq E_{\vec{p}(n)}/m$. Now, note that $E_{\vec{p}}(n)$ is decreasing in each p_k for $p_k \geq 0$, then it is clear that $E_{\vec{p}}(n) \leq E_{\vec{1}}(n)/\min_k p_k$. On the other hand, it is easy to compute by direct probabilistic calculation that $E_{\vec{1}/n}(n) = nh_n$. We conclude by noting that, by (15), $cE_{c\vec{p}}(n) = E_{\vec{p}}(n)$ for any $c > 0$. \square

We now directly use these results to bound the bottleneck distance.

Theorem 1. Let (Z, d_Z) be a smooth compact submanifold of \mathbb{R}^d . Given a covering $N_{Z,n}^{(R,s)}$ of Z with separation $s > 0$ and a number $p \in (0, 1)$, there exists a positive integer $m = m_n(p)$ such that if $\mathbb{Z}_m = \{z_k\}_{k=1}^m$ is a sequence of i.i.d. points sampled uniformly from Z , with probability p one can find a set of n different indices $\{i_1, \dots, i_n\} \subset \{1, \dots, m\}$ with

$$d_B^Z(N_{Z,n}^{(R,s)}, \{z_{i_1}, \dots, z_{i_n}\}) \leq R \quad \text{and} \quad Z = \bigcup_{k=1}^n B_Z(z_{i_k}, 2R).$$

Moreover,¹³

$$m_n(p) \leq \left\lceil \frac{h_n}{\min_z \mathbf{a}(B_Z(z, s/2))} \frac{\mathbf{a}(Z)}{1-p} \right\rceil + 1.$$

This result can also be seen the other way around: For a given m , the probability of finding the aforementioned subset in \mathbb{Z}_m is $P_{\vec{p}_Z}(n, m)$ as given by (14), for suitably defined \vec{p}_Z . The precise form of \vec{p}_Z can be understood from the proof.

Proof. Let $N_{Z,n}^{(R,s)} = \{\widehat{z}_1, \dots, \widehat{z}_n\}$. We consider the coupon-collecting problem in which the k th coupon has been acquired at least once if $\#\{\mathbb{Z}_m \cap V_k\} \geq 1$, where V_k is the k th cell of the Voronoi partition corresponding to the covering net $N_{Z,n}^{(R,s)}$. The components of the probability vector \vec{p} are given by $p_k = \mathbf{a}(V_k)/\mathbf{a}(Z)$ for $k = 1, \dots, n$. Using the fact that (14) is increasing in the number of trials m ,¹⁴ we see that given p we can find a positive integer M such that, for $m \geq M$,

$$\mathbf{P}\left(\bigcap_{k=1}^n \{\#\{\mathbb{Z}_m \cap V_k\} \geq 1\}\right) \geq p.$$

Discarding points when more than one has been found inside the same V_k , we can

¹³ For real x , $[x]$ stands for the largest integer not greater than x .

¹⁴ Something obvious for which, in principle, we do not need to know the exact expression (14).

obtain with probability at least p , exactly one point inside each V_k . Let i_1, \dots, i_n be indices such that $z_{i_k} \in V_k$ for $k = 1, \dots, n$. Then $d_{\mathcal{B}}^Z(\{z_{i_1}, \dots, z_{i_n}\}, N_{Z,n}^{(R,s)}) \leq \max_{z \in \tilde{A}_k} d_Z(z, \hat{z}_k)$, since by Lemma 1, $V_k \subseteq B_Z(\hat{z}_k, R)$, and this concludes the proof of the first claim. Also, by the very same steps plus the triangle inequality we prove that $\{z_{i_1}, \dots, z_{i_n}\}$ constitutes a $2R$ -covering of Z . Finally, note that by Corollary 3, $P_{\tilde{p}}(n, m) \geq p$ for $m \geq h_n/(1-p) \min_k p_k$. Since again by Lemma 1, $\mathbf{a}(V_k) \geq \min_{z \in Z} \mathbf{a}(B_Z(z, s/2))$ the last claim follows. \square

Corollary 4. *Let X and Y be compact submanifolds of \mathbb{R}^d . Let $N_{X,n}^{(R,s)}$ be a covering of X with separation s such that for some positive constant c , $s - 2d_{\mathcal{GH}}(X, Y) > c$. Then, given any number $p \in (0, 1)$, there exists a positive integer $m = m_n(p)$ such that, if $\mathbb{Y}_m = \{y_k\}_{k=1}^m$ is a sequence of i.i.d. points sampled uniformly from Y , we can find, with probability at least p , a set of n different indices $\{i_1, \dots, i_n\} \subset \{1, \dots, m\}$ such that*

$$d_{\mathcal{I}}(N_{X,n}^{(R,s)}, \{y_{i_1}, \dots, y_{i_n}\}) \leq 3d_{\mathcal{GH}}(X, Y) + R$$

and

$$Y = \bigcup_{k=1}^n B_Y(y_{i_k}, 2(R + 2d_{\mathcal{GH}}(X, Y))).$$

Moreover,

$$m_n(p) \leq \left\lceil \frac{h_n}{\min_y \mathbf{a}(B_Y(y, c/2))} \frac{\mathbf{a}(Y)}{1-p} \right\rceil + 1.$$

Proof. Let $\eta = d_{\mathcal{GH}}(X, Y)$. Following Remark 6, we can find an $(R + 2\eta, s - 2\eta)$ n -covering of Y , which we denote by $N_{Y,n}^{(\tilde{R}, \tilde{s})}$, such that $d_{\mathcal{I}}(N_{X,n}^{(R,s)}, N_{Y,n}^{(\tilde{R}, \tilde{s})}) \leq \eta$. Let, as in Theorem 1, $m = m_n(p)$ be such that for any i.i.d. set of points $\mathbb{Y}_m = \{y_1, \dots, y_m\}$ uniformly sampled from Y one has

$$\mathbf{P}(\exists \{y_{i_1}, \dots, y_{i_n}\} \subset \mathbb{Y}_m : d_{\mathcal{B}}^Y(N_{Y,n}^{(\tilde{R}, \tilde{s})}, \{y_{i_1}, \dots, y_{i_n}\}) \leq \tilde{R}) \geq p,$$

where i_1, \dots, i_n are different indices. Let $N_{Y,n} \subset Y$ be a set of n different points. Then, using the triangle inequality

$$\begin{aligned} d_{\mathcal{I}}(N_{X,n}^{(R,s)}, N_{Y,n}) &\leq d_{\mathcal{I}}(N_{X,n}^{(R,s)}, N_{Y,n}^{(\tilde{R}, \tilde{s})}) + d_{\mathcal{I}}(N_{Y,n}, N_{Y,n}^{(\tilde{R}, \tilde{s})}) \\ &\leq \eta + d_{\mathcal{B}}^Y(N_{Y,n}, N_{Y,n}^{(\tilde{R}, \tilde{s})}). \end{aligned}$$

Hence we obtain, by Theorem 1,

$$\mathbf{P}(\exists N_{Y,n} \subset \mathbb{Y}_m : d_{\mathcal{I}}(N_{X,n}^{(\tilde{R}, \tilde{s})}, N_{Y,n}) \leq \eta + \tilde{R}) \geq p.$$

The other claims follow just as in the proof of Theorem 1. \square

Remark 7.

- (1) The preceding corollary deals with the case of positive detection: X and Y are *nearly isometric* and we wish to detect this by only accessing the point clouds. The constant c quantifies this metric proximity as encoded by the phrase “*nearly isometric*.” For instance, for a recognition task, where for any two *similar* objects X and Y , $d_{\mathcal{GH}}(X, Y) \leq \eta_{\max}$, one could choose $c = s - 2\eta_{\max}$.
- (2) Note that the probability $P_{\tilde{p}_Y}(n, m)$ itself (or $m_n(p)$) depends on $d_{\mathcal{GH}}(X, Y)$ through the constant c , see an example of the application of these ideas in Section 3.4 below.

Note also that one can write the following useful bound

$$P_{\tilde{p}_Y}(n, m) \geq 1 - \frac{h_n}{m \cdot \min_{y \in Y} \mathbf{a}(B_Y(y, \frac{c}{2}))} \mathbf{a}(Y) \quad (16)$$

which was implicitly used in the proof of Theorem 1. It is sensible to assume that one is interested in performing the recognition/classification task for a number of objects which satisfy certain conditions, that is, tune the framework to a particular class of objects. In particular, suppose the class is characterized, among other conditions, by an upper bound on the sectional curvatures. For small $r > 0$ this allows us, via the Bishop–Günther theorem, to obtain a lower bound on $\min_z \mathbf{a}(B_Z(z, r))$ valid *for all* objects Z in the class. This in turn can be used to calibrate the system to provide any prespecified probability p as in Corollary 4 for any two objects within the class, see Section 3.4 and Section 3.2 for a more detailed presentation of these ideas.

A rougher estimate of the value of $m_n(p)$ alluded to in Corollary 4 can be obtained using the value of $E_{\tilde{p}}(n)$ corresponding to the case when all the coupons are equally likely: $m \simeq E_{1/n}(n) = n \cdot h_n \simeq n \log n$.

This concludes the main theoretical foundation of our proposed framework. Now we must devise a computational procedure which allows us to actually find the subset $N_{Y,n}$ inside the given point cloud \mathbb{Y}_m when it exists, or at least to find it with a large probability. Note that in practice we can only access metric information, that is, interpoint distances. A stronger result in the same spirit of Theorem 1 should take into account possible self-isometries of X (Y), which would increase the probability of finding a net which achieves a small $d_{\mathcal{T}}$ distance to the fixed one. We present such a computational framework next.

3. Computational Foundations

There are a number of additional issues that must be dealt with in order to develop an algorithmic procedure from the theoretical results previously presented. These are now addressed.

3.1. Initial Considerations

In practice our input consists of two statistically independent point clouds \mathbb{X}_m and $\mathbb{Y}_{m'}$ each of them composed of i.i.d. points sampled uniformly from X and Y , respectively. For a positive integer $n \ll \min(m, m')$ we construct good coverings $N_{X,n}^{(R,s)}$ of X and $N_{Y,n}^{(R',s')}$ of Y , respectively. Actually, R, s, R' , and s' all depend on n , and we should choose n such that R and R' are small enough to make our bounds useful, see the additional computations below. Details on how we construct these coverings are provided in Section 3.3. We will assume, without loss of generality, that these coverings are statistically independent of \mathbb{X}_m and $\mathbb{Y}_{m'}$.

It is convenient to introduce the following additional notation: For a set of points $\mathbb{Z}_q = \{z_k\}_{k=1}^q$ and for a set of indices $I_u = \{i_1, \dots, i_u\} \subset \{1, \dots, q\}$, let $\mathbb{Z}_q[I_u]$ denote the subset $\{z_{i_1}, \dots, z_{i_u}\}$ of \mathbb{Z}_q .

Corollary 4 suggests that in practice we compute the following symmetric expression:

$$d_{\mathcal{F}}(\mathbb{X}_m, \mathbb{Y}_{m'}) := \max \left(\min_{J_n \subset \{1, \dots, m\}} d_{\mathcal{I}}(N_{X,n}^{(R,s)}, \mathbb{Y}_{m'}[J_n]), \min_{I_n \subset \{1, \dots, m\}} d_{\mathcal{I}}(N_{Y,n}^{(R',s')}, \mathbb{X}_m[I_n]) \right), \quad (17)$$

which depends not only on \mathbb{X}_m and $\mathbb{Y}_{m'}$ but also on prespecified covering nets $N_{X,n}^{(R,s)}$ and $N_{Y,n}^{(R',s')}$. However, we prefer to omit this dependence in the list of arguments in order to keep the notation simpler.

Then, $d_{\mathcal{F}}(\mathbb{X}_m, \mathbb{Y}_{m'})$ roughly upper bounds $d_{\mathcal{GH}}(\mathbb{X}_m, \mathbb{Y}_{m'})$, something we need to require. In fact, for any $I_n \subset \{1, \dots, m\}$, using the triangle inequality for $d_{\mathcal{GH}}$ (Property 1 from Proposition 1), and then Property 3 from Proposition 1:

$$\begin{aligned} d_{\mathcal{GH}}(\mathbb{X}_m, \mathbb{Y}_{m'}) &\leq d_{\mathcal{GH}}(\mathbb{X}_m, \mathbb{X}_m[I_n]) + d_{\mathcal{GH}}(\mathbb{X}_m[I_n], \mathbb{Y}_{m'}) \\ &\leq d_{\mathcal{GH}}(\mathbb{X}_m, \mathbb{X}_m[I_n]) + d_{\mathcal{GH}}(\mathbb{X}_m[I_n], N_{Y,n}^{(R',s')}) + d_{\mathcal{GH}}(N_{Y,n}^{(R',s')}, \mathbb{Y}_{m'}) \\ &\leq d_{\mathcal{H}}^X(\mathbb{X}_m, \mathbb{X}_m[I_n]) + d_{\mathcal{I}}(\mathbb{X}_m[I_n], N_{Y,n}^{(R',s')}) + R'. \end{aligned}$$

Now, considering I_n^* such that

$$d_{\mathcal{I}}(\mathbb{X}_m[I_n^*], N_{Y,n}^{(R',s')}) = \min_{I_n \subset \{1, \dots, m\}} d_{\mathcal{I}}(N_{Y,n}^{(R',s')}, \mathbb{X}_m[I_n]),$$

we find

$$d_{\mathcal{GH}}(\mathbb{X}_m, \mathbb{Y}_{m'}) \leq d_{\mathcal{H}}^X(\mathbb{X}_m, \mathbb{X}_m[I_n^*]) + d_{\mathcal{F}}(\mathbb{X}_m, \mathbb{Y}_{m'}) + R'.$$

Symmetrically, we also obtain for J_n^* such that

$$d_{\mathcal{I}}(\mathbb{Y}_{m'}[J_n^*], N_{X,n}^{(R,s)}) = \min_{J_n \subset \{1, \dots, m'\}} d_{\mathcal{I}}(N_{X,n}^{(R,s)}, \mathbb{Y}_{m'}[J_n]),$$

$$d_{\mathcal{GH}}(\mathbb{X}_m, \mathbb{Y}_{m'}) \leq d_{\mathcal{H}}^Y(\mathbb{Y}_{m'}, \mathbb{Y}_{m'}[J_n^*]) + d_{\mathcal{F}}(\mathbb{X}_m, \mathbb{Y}_{m'}) + R.$$

Hence, combining the last two expressions

$$\begin{aligned} d_{\mathcal{GH}}(\mathbb{X}_m, \mathbb{Y}_{m'}) &\leq d_{\mathcal{F}}(\mathbb{X}_m, \mathbb{Y}_{m'}) \\ &\quad + \min(d_{\mathcal{H}}^X(\mathbb{X}_m, \mathbb{X}_m[I_n^*]), d_{\mathcal{H}}^Y(\mathbb{Y}_{m'}, \mathbb{Y}_{m'}[J_n^*])) \\ &\quad + \max(R, R'), \end{aligned} \quad (18)$$

which implies (Corollary 1) a similar upper bound for $d_{\mathcal{GH}}(X, Y)$. In fact, let $r_m := d_{\mathcal{H}}^X(X, \mathbb{X}_m)$ and let $r_{m'} := d_{\mathcal{H}}^Y(Y, \mathbb{Y}_{m'})$, then

$$\begin{aligned} d_{\mathcal{GH}}(X, Y) &\leq d_{\mathcal{F}}(\mathbb{X}_m, \mathbb{Y}_{m'}) \\ &\quad + \min(d_{\mathcal{H}}^X(\mathbb{X}_m, \mathbb{X}_m[I_n^*]), d_{\mathcal{H}}^Y(\mathbb{Y}_{m'}, \mathbb{Y}_{m'}[J_n^*])) \\ &\quad + \max(R, R') + r_m + r_{m'}. \end{aligned} \quad (19)$$

Let $\Delta_X := d_{\mathcal{H}}^X(\mathbb{X}_m, \mathbb{X}_m[I_n^*])$ and let $\Delta_Y := d_{\mathcal{H}}^Y(\mathbb{Y}_{m'}, \mathbb{Y}_{m'}[J_n^*])$.

We now deal with the opposite kind of inequality. By Corollary 4 we know that with probability at least $P_{\tilde{p}_X}(n, m) \times P_{\tilde{p}_Y}(n, m')$ we will have both¹⁵

$$d_{\mathcal{F}}(\mathbb{X}_m, \mathbb{Y}_{m'}) \leq 3d_{\mathcal{GH}}(X, Y) + \max(R, R') \quad (20)$$

and

$$\Delta_X \leq 2(R' + 2d_{\mathcal{GH}}(X, Y)) \quad \text{and} \quad \Delta_Y \leq 2(R + 2d_{\mathcal{GH}}(X, Y)), \quad (21)$$

and from this it follows, in particular, that $\min(\Delta_X, \Delta_Y) \leq 2\max(R, R') + 4d_{\mathcal{GH}}(X, Y)$ with the same probability.

Summing up, we have thus obtained

$$\begin{aligned} d_{\mathcal{GH}}(X, Y) - \alpha(R, R', m, m') &\leq \mathcal{L}(\mathbb{X}_m, \mathbb{Y}_{m'}) \\ &\stackrel{\text{prob}}{\leq} 7(d_{\mathcal{GH}}(X, Y) + \beta(R, R')), \end{aligned} \quad (22)$$

where the symbol $\stackrel{\text{prob}}{\leq}$ means that the inequality holds with probability $P_{\tilde{p}_X}(n, m) \times P_{\tilde{p}_Y}(n, m')$, $\alpha(R, R', m, m') := \max(R, R') + (r_m + r_{m'})$,¹⁶ $\beta(R, R') := \frac{3}{7}\max(R, R')$, and

$$\mathcal{L}(\mathbb{X}_m, \mathbb{Y}_{m'}) := d_{\mathcal{F}}(\mathbb{X}_m, \mathbb{Y}_{m'}) + \min(\Delta_X, \Delta_Y). \quad (23)$$

Note, for future reference, that $\mathcal{L}(\mathbb{X}_m, \mathbb{Y}_{m'}) \leq \frac{3}{2}\max(\mathbf{diam}(X), \mathbf{diam}(Y))$.

Remark 8. Note that α , β , and the probability can be controlled by suitably choosing all the parameters. We have therefore obtained an expression like the one anticipated in Section 2.1, eq. (7). The main difference is that we have not yet proved that $\mathcal{L}(\mathbb{X}_m, \mathbb{Y}_{m'})$ can be computed exactly or approximately in practice. In Section 3.6 we present a simple algorithm for approximately computing this quantity. We do not provide bounds on the fidelity of the algorithm in this paper. Results in this direction are subject of current efforts.

¹⁵ Because we assumed \mathbb{X}_m to be independent of $\mathbb{Y}_{m'}$.

¹⁶ Observe that $\alpha(R, R', m, m') \leq 3\max(R, R')$.

Remark 9. By a modification of the ideas presented here it may be possible to provide a framework recognition of partial objects: One might want to check whether one object is a part of another one. Clearly, in that case, one should simply compute one of the two expressions inside the $\max(,)$ defining $d_{\mathcal{F}}$ (17). The covering net $N_{Y,n}^{(R',s')}$ should represent the object that we want to find inside the one represented by \mathbb{X}_m .

3.2. Working with Point Clouds

All we have are finite sets of points (point clouds) sampled from each metric space, and all our computations must be based on *these observations* only. Since we made the assumption of randomness in the sampling (and it also makes sense in general to make a random model of the problem, given that the shapes are acquired by a scanner for example), we must relate the number of acquired data points to the coverage properties we wish to have. In other words, and following our theory above, we would like to say that given a desired probability p_c and radius r_c , there exists a finite m such that the probability of covering all the metric spaces with m balls (intrinsic or not) of radius r_c centered at those m random points is at least p_c . These kinds of characterizations are easy to deal with in the case of submanifolds of \mathbb{R}^d , where the *tuning* comes from the curvature bounds available. For this we follow [42]. Let Z be a smooth and compact submanifold of \mathbb{R}^d of dimension k . Let $\mathbb{Z}_m = \{z_1, \dots, z_m\} \subset Z$ consist of m i.i.d. points uniformly sampled from Z . For $r > 0$, define

$$f_Z(r) := \min_{z \in Z} \mathbf{a}(B_Z(z, r)). \quad (24)$$

Then, for $p \in (0, 1)$ and $\delta > 0$, we can prove that if $m \geq -\log((1 - p) f_Z(\delta/4)) / f_Z(\delta/2)$, then

$$p_{\delta,m} := \mathbf{P}\left(Z \subseteq \bigcup_{i=1}^m B_Z(z_i, \delta)\right) \geq p. \quad (25)$$

The function f_Z can be lower bounded using an upper bound, K , for the sectional curvatures of Z (the Bishop-Günther theorem, see [24]): $f_Z(r) \geq F_{K,k}(r)$ where $F_{K,k}(r)$ denotes the area of a ball of radius r in a space of constant sectional curvature K and dimension k . For example, when $K > 0$, one has

$$F_{K,k}(r) = \frac{2\pi^{k/2}}{\Gamma(k/2)} \int_0^r \left(\frac{\sin(t\sqrt{K})}{\sqrt{K}} \right)^{k-1} dt.^{17}$$

This relation gives us some guidance about the number points we must sample in order to have a certain covering radius, or to estimate the covering radius in terms of m . An important point to note is that this kind of relation, (25), should hold for

¹⁷ $\Gamma(t)$ denotes the usual *Gamma* function: $\Gamma(t) = \int_0^\infty u^{t-1} e^{-u} du$.

the family of shapes we want to work with (in a way similar to the one shown in Section 3.4), therefore, once given bounds on the curvatures that characterize the family, one can determine a precise probabilistic covering relation for it. We leave the exploitation/application of this idea for future work.

Given the natural number $n \leq m$ (or, eventually, $s > 0$), we use the procedure described in Section 3.3 below to find n -points from \mathbb{Z}_m which constitute a covering of \mathbb{Z}_m of the given cardinality n (or of the given separation s or given covering radius R) and of the resulting radius R_{res} (or resulting separation s_{res}). We denote this set by $N_{\mathbb{Z}_m, n}^{(R_{\text{res}}, s)} \subseteq \mathbb{Z}_m$ (or $N_{\mathbb{Z}_m, n}^{(R, s_{\text{res}})} \subseteq \mathbb{Z}_m$, respectively).

3.3. Finding Coverings

In order to find the coverings $N_{\mathbb{Z}_m, n}^{(R, s)}$, we use the well-known Farthest Point Sampling (FPS) strategy, which we describe next. Suppose we have a dense sampling \mathbb{Z}_m of the smooth and compact submanifold (Z, d_Z) of \mathbb{R}^d as described by the discussion above. We want to simplify our sampling and obtain a well-separated covering net of the space. We also want to estimate the covering radius and separation of our covering net. It is important to obtain subsets which retain as well as possible the metric information contained in the initial point cloud in order to make computational tasks more treatable without sacrificing precision.

We first show a procedure of how to sample the whole of Z . Fix n as the number of points we want to have in our simplified point cloud \mathcal{P}_n . We build \mathcal{P}_n recursively. Given \mathcal{P}_{n-1} , we select $p \in Z$ such that $d_Z(p, \mathcal{P}_n) = \max_{z \in Z} d_Z(z, \mathcal{P}_{n-1})$ (here we consider of course, geodesic distances). There might exist more than one point which achieves the maximum, we either consider all of them or randomly select one and add it to \mathcal{P}_{n-1} . This subsampling procedure has been studied and efficiently implemented in [44] for the case of surfaces represented as point clouds.

The FPS procedure satisfies several useful properties as described below.

Let $M(\mathcal{P}_{n-1}) \subset Z$ denote the set of points z for which $d_Z(\mathcal{P}_{n-1}, z)$ is maximal. We denote by s_n and R_n the separation and covering radius of $\mathcal{P}_n \subset Z$, respectively.

Lemma 3. *Let \mathcal{P}_n be the set obtained for each $n \geq n_0$ according to the FPS strategy starting from \mathcal{P}_{n_0} , and let p_{n+1} denote any point in $M(\mathcal{P}_n)$. Then, for $n \geq n_0$,*

- (1) $d_{\mathcal{H}}^Z(Z, \mathcal{P}_{n+1}) \leq d_{\mathcal{H}}^Z(Z, \mathcal{P}_n)$, that is, $R_{n+1} \leq R_n$.
- (2) $d_Z(p_{n+2}, \mathcal{P}_{n+1}) \leq d_Z(p_{n+1}, \mathcal{P}_n)$.
- (3) $s_n := \min_{1 \leq i < j \leq n} d_Z(p_i, p_j) \geq \min_{1 \leq i < j \leq n+1} d_Z(p_i, p_j) = s_{n+1}$.
- (4) $s_n = d_Z(p_n, \mathcal{P}_{n-1})$.
- (5) $d_{\mathcal{H}}^Z(Z, \mathcal{P}_n) = d_Z(p_{n+1}, \mathcal{P}_n)$.
- (6) $n \leq \mathbf{a}(Z) / f_Z(s_n/2)$ where \mathbf{a} is the area measure on Z and f_Z was defined in (24).¹⁸

¹⁸ Note that with curvature bounds one can obtain a more explicit relation between s_n and n .

In practice we do not have access to Z but only to a point cloud, \mathbb{Z}_m , sampled from it. However, we can still follow the same algorithmic procedure.

Remark 10. These properties make it easy to compute s_n and R_n *on the fly* inside the algorithm, something useful when the objective is to obtain either a prespecified covering radius or a minimal prespecified separation. However, it turns out to be useful to have an estimate on n depending on a prespecified covering radius, that is, we want to find n such that using the FPS we obtain a covering of Z consisting of n points and with radius not greater than ε . Property 6 in Lemma 3 gives us a way. Observe that $s_n = R_{n-1}$, then note that if $n \geq \mathbf{a}(A)/f_Z(\varepsilon/2)$ we must have $f_Z(s_n/2) \leq f_Z(\varepsilon/2)$. But f_Z is obviously nondecreasing, therefore $\varepsilon \geq s_n = R_{n-1} \geq R_n$.

An interesting problem to solve has to do with the behavior of s_n with n through the FPS procedure, in the sense that we would like to know the maximum number of steps of the procedure that can be performed such that the separation remains larger than a prespecified number, check Remark 7. Note, for example, that in the case of the unit sphere, S^2 , the construction of the FPS net goes roughly as follows: The first two points are any antipodal points, call them p_1 and p_2 . The third point can be any on the equator with respect to p_1 and p_2 . The fourth point will also lie on the equator defined by p_1 and p_2 but will be antipodal to p_3 . The next eight points will be the centers of the octants defined by the three maximal circumferences passing through $\{p_1, p_2, p_3, p_4\}$, $\{p_1, p_2, p_5, p_6\}$, and $\{p_3, p_4, p_5, p_6\}$. The construction follows a similar pattern for $n > 8$. We can therefore obtain an exact formula for s_n . Now, given a surface $S \in \mathcal{A}$ (\mathcal{A} is a certain class of compact smooth surfaces), we would like to be able to lower bound $s_n(S)$ by some quantity related to $s_n(S^2)$. Perhaps this will require assuming upper bounds on the Gauss curvature of $S \in \mathcal{A}$. In any case, knowledge of this lower bound will let us find, for any given $s > 0$, an $n_s \in \mathbb{N}$ such that for all $n \leq n_s$, $s_n(S) \geq s$ for all $S \in \mathcal{A}$.

Let us now assume that the discrete metric space (\mathbb{Z}_m, d_Z) is a good random sampling of the underlying (Z, d_Z) in the sense that $d_{\mathcal{H}}(Z, \mathbb{Z}_m) \leq r$ with a certain probability $p_{r,m}$, as discussed in Section 3.2. We then want to simplify \mathbb{Z}_m in order to obtain a set \mathcal{P}_n with n points, which is both a good subsampling and a well-separated covering net of X .¹⁹ We want to use our n sampled points in the best possible way. We are then led to using the construction discussed above. For example, choose randomly one point $p_1 \in \mathbb{Z}_m$ and consider $\mathcal{P}_1 = \{p_1\}$.²⁰ Run the procedure FPS until $n - 1$ other points have been added to the set of points.²¹

¹⁹ One more reason for wanting the subsampling to be well separated, besides the one given by Corollary 4, is that intuitively, the more separated the covering net, the more efficient the use of the points to cover the metric space.

²⁰ Another option is choosing p_1 and p_2 in \mathbb{Z}_m at maximal distance and then recurse.

²¹ As we mentioned before, the goal can be different: Keep adding points while the separation of the resulting subsampling is big enough as measured by some prespecified constant $s > 0$.

Now compute $r_n := \max_{q \in \mathbb{X}_m} d(q, \mathcal{P}_n)$. Then, as with probability $p_{r,m}$, \mathcal{P}_n is an $(r + r_n)$ -covering net of X with separation s_n as expressed in Lemma 3. Following this, we now use the notation $N_{Z,n}^{((r+r_n), s_n)}$.

Next, we present a simplified example of application of the ideas discussed so far.

3.4. An Idealized Example

Suppose, for instance, that we are trying to detect, amongst a finite number of objects $\{X^i\}_{i=1}^L$ belonging to a certain family \mathcal{A} , when two objects are isometric. We will assume for simplicity of exposition that we have only two possible cases or hypotheses: either (H1) $d_{\mathcal{GH}}(X^i, X^j) = 0$; or (H2) $d_{\mathcal{GH}}(X^i, X^j) \geq D$ for some $D > 0$ for all $1 \leq i, j \leq L$.

We characterize the family \mathcal{A} as those smooth compact surfaces of \mathbb{R}^3 such that their Gaussian curvature is bounded from above by some positive constant K , whose total area is bounded from above by some finite constant A . Then, for any sufficiently small $t > 0$,

$$f_S(t) := \min_{x \in S} \mathbf{a}(B_S(x, t)) \geq \frac{2\pi}{K}(1 - \cos(t\sqrt{K})) =: F_{K,2}(t)$$

for all $S \in \mathcal{A}$, by the Bishop–Günther theorem, see Section 3.2. Note, in particular, that $F_{K,2}(t) > 0$ for $0 < t < \pi/\sqrt{K}$.

For $1 \leq i \leq L$ we will denote by $\mathbb{X}_{m_i}^i$ the point cloud corresponding to the object X^i and r_i will denote numbers such that $X \subset B(\mathbb{X}_{m_i}^i, r_i)$.²²

Let X^i and X^j be any two such objects, we will decide, in this example, that X^i and X^j are isometric whenever $\mathcal{L}(\mathbb{X}_{m_i}^i, \mathbb{X}_{m_j}^j)$ is smaller than a certain threshold, see eq. (22).

Fix $\varepsilon > 0$. For all X^i choose coverings $N_{X^i, n_i}^{(R_i, s_i)}$ such that $\max_{1 \leq i \leq L} R_i \leq \varepsilon$, then n_i will be fixed by the procedure one uses to construct these coverings; see Section 3.3. Let $n := \max_i n_i$ and let $R := \min_i R_i \leq \varepsilon$. By adding new points to each of the coverings, if necessary, construct new coverings, all with n points, covering radius ε and the resulting separation s_i . Let $s := \min_i s_i$. Note that we can estimate n in terms of ε , A , and K using the discussion in Remark 10. In fact, $n \geq n_\varepsilon := 1 + \lceil A/F_{K,2}(\varepsilon/2) \rceil$ will do the job.

We are now going to estimate the number of sample points (cardinality of the point clouds) needed for each (all) of the objects in order to be able to detect (H1) with high probability.

According to (22), for any $1 \leq i, j \leq L$, we know that:

- Under (H1), with a probability $Q_{ij} := P_{\tilde{p}_{x_i}}(n, m_i) \times P_{\tilde{p}_{x_j}}(n, m_j)$, we have

$$\mathcal{L}(\mathbb{X}_{m_i}, \mathbb{X}_{m_j}) \leq 3\varepsilon.$$

²² In this example we neglect the fact that this covering relation holds with a certain probability.

- Also, under (H2), assuming $\varepsilon \geq r_k$ for $1 \leq k \leq L$,²³

$$\mathcal{L}(\mathbb{X}_{m_i}, \mathbb{X}_{m_j}) \geq D - 3\varepsilon.$$

This tells us how to design ε in relation to D in order to be able to tell both hypotheses apart by computing $\mathcal{L}(\mathbb{X}_{m_i}, \mathbb{X}_{m_j})$. Thus, let $\varepsilon \ll D/6$.²⁴

Now, one wants to impose Q_{ij} to be high, that is, $Q_{ij} \geq (1 - q)^2$ for some small prespecified q . Then, using the comments in Remark 7, we see we can, for example, fix $c := s$ and estimate the required number of samples for each X_i as $m_i \geq h_n A/q \cdot F_{K,2}(s/2)$. In conclusion, one can require that all the point clouds consist of at least $h_{n_\varepsilon} A/q \cdot F_{K,2}(s/2)$ points (sampled uniformly) from each of the objects and that all the coverings (constructed using FPS) consist of at least n_ε points.

3.5. Computing Geodesic Distances

In our experiments we have always worked with submanifolds of \mathbb{R}^d . We have used a graph-based distance computation following [31], or the exact distance, which can be computed only for certain examples (spheres, planes). We could also use the techniques developed for triangular surfaces in [35], or, this being the optimal candidate, the work on geodesics on (maybe noisy) point clouds developed in [42].

The geodesic computation leads to additional sources of (controllable) errors. We cannot compute $d_X(x_i, x_j)$ and $d_Y(y_i, y_j)$ exactly, but rather approximate values $d_X^h(x_i, x_j)$ and $d_Y^{h'}(y_i, y_j)$ for which error bounds are often available [42]. For some suitable function $f(\cdot, \cdot, \cdot, \cdot)$,

$$|d_X(x_i, x_j) - d_X^h(x_i, x_j)| \leq f(h, r, s, n) \quad (26)$$

and

$$|d_Y(y_i, y_j) - d_Y^{h'}(y_i, y_j)| \leq f(h', r', s', n), \quad (27)$$

where h and h' control the degrees of approximation. These kinds of bounds can be computed for all the approximations we have worked with (see [3], [35]), and also for methods like the one proposed in [42]. We omit in this paper the inclusion of this source of errors in our considerations, results in that direction will be reported elsewhere.

²³ This is reasonable since $\mathbb{X}_{m_i}^i$ are supposed to be finer samplings than $N_{X^i, n}^{(R_i, s_i)}$.

²⁴ Which means that all $R_i \ll D/6$.

3.6. Additional Implementational Details

In this section we conclude the details on the implementation of the framework here proposed. The first step of the implementation is the computation of $d_{\mathcal{F}}$ and, subsequently, \mathcal{L} , which from the theory we described before, bounds the Gromov–Hausdorff distance.

We have implemented a simple algorithm.²⁵ According to the definition of $d_{\mathcal{F}}$, (17), given the matrix of pairwise geodesic distances between points of \mathbb{X}_m , we need to determine whether there exists a submatrix of the whole distance matrix corresponding to \mathbb{X}_m which has a small $d_{\mathcal{I}}$ distance to the corresponding interpoint distance matrix of a given $N_{Y,n}^{(R',s')}$. Since we are free to choose (any coverings), we select this latter covering net as the result of applying the FPS procedure to obtain a subsample consisting of n points, where the first two points are selected to be at maximal distance from each other. We believe that this choice, by the very nature of the FPS sampling procedure, produces a set of points with certain particularly interesting metric characteristics. For example, just to motivate our choice, consider the set of the first seven FPS points of a dense point cloud on a crocodile and a dog models shown in Figure 1.

To fix notation, let $\mathbb{X}_m = \{x_1, \dots, x_m\}$ and let $N_{Y,n}^{(R',s')} = \{y_{j_1}, \dots, y_{j_n}\}$. We then use the following algorithm:

($k = 1, 2$) Choose x_{i_1} and x_{i_2} such that $|d_X(x_{i_1}, x_{i_2}) - d_Y(y_{j_1}, y_{j_2})|$ is minimized.

($k > 2$) Let $x_{i_{k+1}} \in \mathbb{X}_m$ be such that $e_{k+1}(x_{i_{k+1}}) = \min_{1 \leq i_l \leq m} e_{k+1}(x_{i_l})$ where

$$e_{k+1}(x_{i_l}) = \max_{1 \leq r \leq k} |d_X(x_{i_l}, x_{i_r}) - d_Y(y_{j_{k+1}}, y_{j_r})|.$$

We stop when n points, $\{x_{i_1}, x_{i_2}, \dots, x_{i_n}\}$, have been selected and, therefore, a distance submatrix $((d_X(x_{i_u}, x_{i_v})))_{u,v=1}^n$ is obtained.

Since we can write

$$\begin{aligned} d_{\mathcal{I}}(\{x_{i_1}, \dots, x_{i_n}\}, N_{Y,n}^{(R',s')}) &\leq \frac{1}{2} \max_{1 \leq k \leq n} \max_{1 \leq t \leq k-1} |d_X(x_{i_k}, x_{i_t}) - d_Y(y_{j_k}, y_{j_t})| \\ &= \frac{1}{2} \max_{1 \leq k \leq n} e_k(x_{i_k}), \end{aligned}$$

we then see that with our algorithm we are trying to decrease the error by working across the subdiagonal rows of the distance matrix corresponding to $N_{Y,n}^{(R',s')} = \{y_{j_1}, \dots, y_{j_n}\}$.

Of course, we now use the same algorithm to compute the other half of $d_{\mathcal{F}}$. Note that the set of indices $\{i_1, \dots, i_n\}$ corresponds to I_n^* as introduced in the definition of Δ_X and, subsequently, \mathcal{L} , eq. (23). Therefore, we also obtain an approximation to $\mathcal{L}(\mathbb{X}_m, \mathbb{Y}_{m'})$.

²⁵ This simpler algorithm can in turn be modified to be exhaustive and therefore rigorous, details will be provided elsewhere.

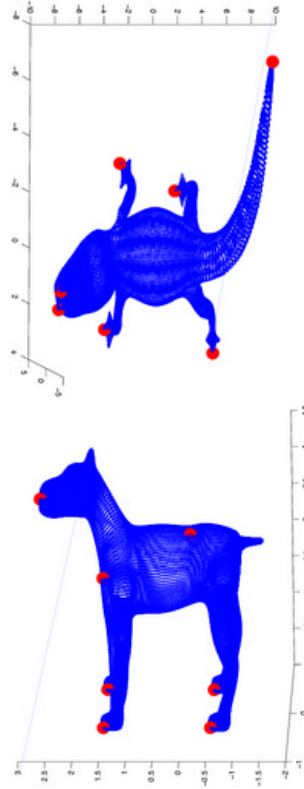


Fig. 1. FPS nets (for $n = 7$) on two point cloud models shown as gray balls. Note the perceptual meaningfulness of the point locations automatically chosen by the procedure.

The case $k = 1, 2$ requires visiting all $m(m - 1)/2$ interpoint distances between points in \mathbb{X}_m . For $k \geq 3$, one must check km different interpoint distances. Then the complexity of the algorithm is $O(2h_n m + m^2)$. We are currently studying computational improvements along with error bounds for the results provided by the algorithm.

Of course, we still have to prove (or disprove) that the above algorithm, based on FPS covering nets, approximates $d_{\mathcal{F}}$ within a reasonable factor. This is the subject of current efforts.

4. Examples

We now present simple experiments that illustrate the application of the theoretical and computational framework introduced in the previous sections. We should note

that in these experiments we don't yet exploit the full potential of our theory.²⁶ For example, to use some of the bounds we need to estimate (or know!) curvature bounds. This estimation could be done using bootstrapping and will be investigated in the future. Also, in the future, we plan to make these experiments more rigorous, including concepts of hypothesis testing.

We complemented the more complex data (as presented below) with simple shapes:

[Plane] $\Sigma_\pi = [-\pi/\sqrt{8}, \pi/\sqrt{8}]^2$ and \mathbb{X}_m are points sampled uniformly from the square. Note that $\text{diam}(X) = \pi$.

[Sphere] $S = \{x \in \mathbb{R}^d : \|x\| = 1\}$ and \mathbb{X}_m is a set of points uniformly distributed on the sphere.

We generated the sample points using the method of Muller, see [46].

4.1. Positive Detection

We first test our framework when X and Y are isometric. We consider $X = Y$ and see whether we make the right decision based on the discrete measurements. Let \mathbb{X}_m and \mathbb{Y}_m be two independent sets composed of m independent, uniformly distributed random points on X . We consider X to be either the plane Σ_π or the sphere S as defined above. Given n , using the FPS procedure, we construct $N_{\mathbb{X}_m, n}^{(R_X, s_X)}$ and $N_{\mathbb{Y}_m, n}^{(R_Y, s_Y)}$ from \mathbb{X}_m and \mathbb{Y}_m , respectively, and look for a metric match inside \mathbb{X}_m and \mathbb{Y}_m , respectively, following the algorithm described in Section 3.6 for the computation of $d_{\mathcal{F}}(\mathbb{X}_m, \mathbb{Y}_m)$ and, subsequently, $\mathcal{L}(\mathbb{X}_m, \mathbb{Y}_m)$.²⁷ For each dataset we tested for values of $m \in M = \{1000, 2000, 2500\}$ and $n \in N = \{20, 40, \dots, 140\}$, and obtained the results reported below. In Tables 1 and 2 we show the values

Table 1. Table with values of \mathcal{L} for $X, Y = P_\pi$ (a plane). See the text for a detailed explanation.

	$m \setminus n$	20	40	60	80	100	120	140
\mathcal{L}	1000	0.57077	0.39095	0.32211	0.29971	0.26287	0.24900	0.24900
	2000	0.57216	0.38335	0.31009	0.28149	0.24506	0.24074	0.22770
	2500	0.56942	0.37424	0.30553	0.26125	0.23818	0.24336	0.22468
$3 \max(R_X, R_Y)$	1000	1.4929	0.96361	0.71275	0.59935	0.51257	0.48078	0.42079
	2000	1.5607	1.0024	0.75905	0.65428	0.53287	0.49245	0.44269
	2500	1.5626	1.0317	0.76530	0.66509	0.54065	0.50211	0.45791
prob \geq	1000	0.83082	0.55117	0.22773	0.044571	*	*	*
	2000	0.91527	0.77526	0.58685	0.44374	0.21043	0.14020	0.039607
	2500	0.93275	0.82145	0.66751	0.56269	0.35018	0.25493	0.13207

²⁶ For instance, we are not taking into account the probability of covering the shape with the random cloud sampled from it, see (25).

²⁷ Keep in mind that actually $d_{\mathcal{F}}(\mathbb{X}_m, \mathbb{Y}_{m'})$ depends on n , see its definition (17).

Table 2. Table with values of \mathcal{L} for $X, Y = S$ (a unit sphere). See the text for a detailed explanation.

	$m \backslash n$	20	40	60	80	100	120	140
\mathcal{L}	1000	0.65513	0.50742	0.44578	0.41879	0.38161	0.36817	0.35826
	2000	0.63882	0.49814	0.43230	0.39641	0.38798	0.34721	0.31449
	2500	0.63873	0.51874	0.40902	0.39149	0.34665	0.32906	0.31931
$3 \max(R_X, R_Y)$	1000	1.7930	1.2932	0.98264	0.87936	0.78162	0.72061	0.64876
	2000	1.8154	1.3407	1.0688	0.91887	0.83075	0.72182	0.66511
	2500	1.8154	1.3573	1.0264	0.91894	0.79693	0.72379	0.68160
prob \geq	1000	0.71395	0.39766	0.085661	0.0017990	*	*	*
	2000	0.82951	0.68052	0.43286	0.31059	0.16894	0.061612	0.0087141
	2500	0.87192	0.71880	0.52749	0.43477	0.27696	0.16941	0.10045

obtained for \mathcal{L} for values of $m \in M$ and $n \in N$. As expected, the values of \mathcal{L} are small both when compared to the values reported in the next section (for non-isometric shapes, $X = \Sigma_\pi$ and $Y = S$) and when compared to the upper bound $3\pi/2 \simeq 4.7124$, as mentioned after eq. (22). Note that as a verification, in accordance with formula (22) for $d_{\mathcal{GH}}(X, Y) = 0$, we also display the corresponding values of $3 \max(R_X, R_Y)$ and the probability, $P_{\tilde{p}_X}(n, m) \times P_{\tilde{p}_Y}(n, m)$, of having $\mathcal{L} \leq 3 \max(R_X, R_Y)$ estimated by using the bound (16). Asterisks (*) in the tables denote that our lower bound (16) was not tight enough to give a positive number. Note that in our experiments we always obtained $\mathcal{L} \leq 3 \max(R_X, R_Y)$. This is in some sense a validation of our algorithm for computing \mathcal{L} . It also can be interpreted that there is still room for improvement in the bounds (22).

4.2. Positive Rejection

We now proceed to compare shapes that are not isometric. We let $X = \Sigma_\pi$ (a plane) and $Y = S$ (a sphere). In this case we expect to be able to detect, based on the finite point clouds, that \mathcal{L} is large, in comparison to the values we obtained in the previous section, when the shapes were actually the same.

Table 3 shows the results of a simulation in which we compared the sphere S and the plane Σ_π , while varying the covering net sizes and the total number of points uniformly sampled from them ($n \in N$ and $m \in M$ as before). As expected, the values are larger than when comparing plane against plane or sphere against sphere.

Table 3. Values of \mathcal{L} for a comparison between Σ_π and S for $n \in N$ and $m \in M$.

	$m \backslash n$	20	40	60	80	100	120	140
\mathcal{L}	1000	1.3191	1.2715	1.1583	1.1739	1.1919	1.1537	1.0849
	2000	1.0751	1.0751	1.0816	1.0991	1.1155	1.1155	1.1305
	2500	1.2059	1.1369	1.1369	1.1471	1.0984	1.1179	1.1179

4.3. *Three-Dimensional Shape Recognition*

We conclude the experiments with real (more complex) data. We have four sets (isometry classes) of shapes,²⁸ the crocodile $C = \{C_1, C_2\}$, the giraffe $G = \{G_1, G_2\}$, the hand $H = \{H_1, H_2\}$, and the body, $B = \{B_1, B_2\}$. The two shapes in each set are bends of each other and therefore isometric. We ran the algorithm with $n = 50$, $m = 2500$ (recall the rough estimate $m \simeq n \log n$ given in Remark 7 and note that with this choice $n \log n \simeq 200 \ll 2500 = m$), using Dijkstra's algorithm to compute geodesic distances.²⁹ The data description and results are reported in Figure 2. Observe that for any fixed shape $X \in C \cup G \cup H \cup B$, the value of $\mathcal{L}(X, Y)$ is always lower for Y in the same isometry class as X . We note that the technique is not only able to discriminate between different objects but, as expected, doesn't get confused by bends: The distances between a given object and the possible bends of another one are very similar, as should be the case for isometry invariant recognition.

5. Extensions and Conclusions

The comparison framework introduced here opens the doors to extensive research in the area. We conclude this paper by presenting some possible directions.

5.1. *Extensions*

The extension to more general metric spaces can be done, in principle, once one agrees upon some definition of uniform probability measure, something that could be done using the Hausdorff measure, which is defined from the metric.

Another related possible (and easy) extension is that of admitting the points to be sampled from the manifolds with probability measures other than uniform. Actually, in the case of surfaces in \mathbb{R}^3 acquired by a three-dimensional scanner, the probability measure models the acquisition process itself. In this case, the framework here presented can be extended for a wide family of probability measures, namely those which admit a density function which vanishes at most in sets of 0-uniform measure, i.e., there are no *holes* in the acquisition process.

In other situations, it might make more sense to consider the recognition problem for triplets (X, d, μ) , where (X, d) is a metric space and μ is a (probability) measure defined on sets of X .

²⁸ The datasets were kindly provided for us by Professor Kimmel and his group at the Technion.

²⁹ We first considered 10,000 points sampled from each of the objects. From each of these sets we then subsampled the 2500 we worked with. For each dataset we used the 10,000 points to construct a 15-nearest neighbors graph and then computed the intrinsic distance matrix between the 2500 subset of points using Dijkstra's algorithm over the whole graph.



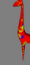







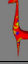





Model								
	1.4071	5.5900	11.769	10.776	11.109	11.111	11.109	11.146
	5.5900	1.4576	12.647	10.196	11.119	11.120	11.123	11.159
	11.769	12.647	1.9357	6.2874	15.169	15.170	15.274	15.207
	10.776	10.196	6.2874	2.0342	14.692	14.693	14.797	14.746
	11.109	11.119	15.169	14.692	0.0045257	0.019845	0.22663	0.19691
	11.111	11.120	15.170	14.693	0.019845	0.0047940	0.23164	0.19715
	11.109	11.123	15.274	14.797	0.22663	0.23164	0.033033	0.096958
	11.146	11.159	15.207	14.746	0.19691	0.19715	0.096958	0.032846
Diameters	22.205	22.222	30.322	29.367	0.040326	0.038832	0.44957	0.37998

Fig. 2. Comparison results for the complex objects described in Section 4.3. The number of points per model are indicated in the first row under the corresponding figure. The values reported are the estimate of \mathcal{L} between all pairs of objects given by our algorithm. Note that: (1) for any object X in this experiment, $\mathcal{L}(X, Y)$ is minimal for Y in the isometry class of X ; and (2) all objects within the same isometry class have similar values of \mathcal{L} with all other objects belonging to another class.

An interesting extension which might make the computational analysis easier would be working with alternative definitions of Hausdorff distance. For example, remembering that the Hausdorff distance between $X, Y \subset Z$, (Z, d, μ) a metric space with metric d (and with probability measure μ), was defined as

$$d_{\mathcal{H}}^Z(X, Y) := \max \left(\sup_{x \in X} d(x, Y), \sup_{y \in Y} d(y, X) \right).$$

Then one can consider substituting each of the suprema inside the $\max(\cdot, \cdot)$ operation by an L_p -approximation (for $p \geq 1$), for example, $\sup_{x \in X} d(x, Y) \leftrightarrow (\int d^p(x, Y) \mu(dx))^{1/p}$, and similarly for the other supremum to obtain, also allowing for an L_q -approximation of the $\max(q \geq 1)$:

$$d_{\mathcal{H}_{p,q}}^Z(X, Y) := \left(\left(\int d^p(x, Y) \mu(dx) \right)^{q/p} + \left(\int d^p(y, X) \mu(dy) \right)^{q/p} \right)^{1/q}$$

and then the corresponding notion of the (p, q) -Gromov–Hausdorff distance is accordingly defined. In particular, it would be interesting to know the corresponding

(p, q) version of Property 5 of Proposition 1. Of particular interest in this respect is the very recent work [53].

5.1.1. Scale-Dependent Comparisons. In some applications it might be interesting to compare objects in a more local fashion or, in other words, in a scale-dependent way. For example, given two objects \mathcal{S}_1 and \mathcal{S}_2 (with corresponding geodesic distance functions d_1 and d_2) one might wonder whether they resemble each other under the distance $d_{\mathcal{GH}}(\cdot, \cdot)$ when each of them is endowed with the metric $d_i^\varepsilon := \varepsilon(1 - e^{-d_i/\varepsilon})$, $i = 1, 2$. This choice for the new metrics imposes a scale-dependent comparison.

This situation has an important consequence: When ε is small enough one might choose to replace d_i by their Euclidean counterparts since, for nearby points x and x' on the submanifold $\mathcal{S} \subset \mathbb{R}^k$, $d_{\mathcal{S}}(x, x') \simeq d_{\mathbb{R}^k}(x, x')$. This dispenses with the computational burden of having to approximate the geodesic distance. Also, in a similar vein, in certain applications it may make sense to normalize the distance matrices of all the objects so as to obtain a scale invariant comparison.

5.2. Conclusions

A theoretical and computational framework for comparing (smooth, connected, and compact) submanifolds of \mathbb{R}^d given as point clouds was introduced in this paper. The theoretical component is based on the Gromov–Hausdorff distance, which has been embedded in a probabilistic framework to deal with point clouds and computable discrete distances. Examples illustrating this theory were provided.

We are currently working on proving the correctness of the algorithm described in Section 3.6, improving its computational efficiency, performing additional experiments adding hypotheses testing techniques and, in particular, comparing high-dimensional point clouds with data from image sciences and neuroscience. These further results and extensions will be reported elsewhere.

Acknowledgments

We thank Professor Omar Gil, Professor Ron Kimmel, and Professor Ofer Zeitouni for stimulating conversations on the subject of this paper. A. Elad and R. Kimmel provided valuable data for the experiments. We also thank the anonymous reviewers who helped to improve the presentation of the paper. This work is supported in part by the Office of Naval Research, the National Science Foundation, the National Institutes of Health, the National Geospatial Intelligence Agency, and DARPA. Part of this work was done while Facundo Mémoli was visiting IPAM. The work of Facundo Mémoli is partly supported by CSIC-Uruguay.

References

- [1] E. Arias-Castro, D. Donoho, and X. Huo, Near-optimal detection of geometric objects by fast multiscale methods, Stanford Statistics Department, Technical Report, 2003.
- [2] M. Belkin and P. Niyogi, Laplacian eigenmaps for dimensionality reduction and data representation, University of Chicago CS TR-2002-01, 2002.
- [3] M. Bernstein, V. de Silva, J. Langford, and J. Tenenbaum, Graph approximations to geodesics on embedded manifolds, <http://isomap.stanford.edu/BdSLT.ps>
- [4] J. Borwein and O. Hijab, <http://www.siam.org/journals/problems/downloadfiles/99-5sii.pdf>
- [5] J.-D. Boissonnat and F. Cazals, Coarse-to-fine surface simplification with geometric guarantees, in *EUROGRAPHICS '01*, Manchester (A. Chalmers and T.-M. Rhyne, eds.), 2001.
- [6] I. Borg and P. Groenen, *Modern Multidimensional Scaling, Theory and Applications*, Springer Series in Statistics, Springer-Verlag, New York, 1997.
- [7] M. Botsch, A. Wiratanaya, and L. Kobbelt, Efficient high quality rendering of point sampled geometry, *EUROGRAPHICS Workshop on Rendering*, 2002.
- [8] M. Boutin and G. Kemper, On reconstructing n -point configurations from the distribution of distances or areas, *Adv. Appl. Math.* **32**(4) (2004) 709–735.
- [9] A. Bronstein, M. Bronstein, A. Spira, and R. Kimmel, Face recognition from facial surface metric, *Proc. ECCV* (Part II), 2004, pp. 225–237.
- [10] D. Burago, Y. Burago, and S. Ivanov, *A Course in Metric Geometry*, Graduate Studies in Mathematics, Vol. 33, American Mathematical Society, Providence, RI, 2001.
- [11] D. Burago and B. Kleiner, Separated nets in Euclidean space and Jacobians of bi-Lipschitz maps, *Geom. Funct. Anal.* **8** (1998), 273–282.
- [12] D. Burago and B. Kleiner, Rectifying separated nets, *Geom. Funct. Anal.* **12** (2002), 80–92.
- [13] G. Carlsson, A. Collins, L. Guibas, and A. Zomorodian, Persistent homology and shape description I, Preprint, Stanford Mathematics Department, September 2003.
- [14] G. Charpiat, O. Faugeras, and R. Keriven, Shape metrics, warping, and statistics, *Proc. International Conference on Image Processing*, IEEE Signal Processing Society, New York, 2003.
- [15] T. K. Dey, J. Giesen, and J. Hudson, Decimating samples for mesh simplification, *Proc. 13th Canadian Conference on Computational Geometry*, CCCG, Ottawa, ON, 2001, 85–88, <http://cccg.ca/proceedings/2001>.
- [16] D. L. Donoho and C. Grimes, When does ISOMAP recover the natural parametrization of families of articulated images?, Technical Report 2002-27, Department of Statistics, Stanford University, 2002.
- [17] D. L. Donoho and C. Grimes, Hessian eigenmaps: New locally-linear embedding techniques for high-dimensional data, Technical Report, Department of Statistics, Stanford University, 2003.
- [18] N. Dyn, M. S. Floater, and A. Iske, Adaptive thinning for bivariate scattered data, *J. Comput. Appl. Math.* **145**(2) (2002), 505–517.
- [19] A. Elad (Elbaz) and R. Kimmel, Bending invariant representations for surfaces, *Proc. CVPR'01, Hawaii, Dec. 2001*, IEEE Computer Society, Washington DC, 2001.
- [20] W. Feller, *An Introduction to Probability Theory and its Applications*, Wiley, New York, 1971.
- [21] M. S. Floater and A. Iske, Thinning algorithms for scattered data interpolation, *BIT Numer. Math.* **38** (1998), 705–720.
- [22] J. Giesen and U. Wagner, Shape dimension and intrinsic metric from samples of manifolds with high co-dimension, *ACM Symposium on Computational Geometry, San Diego, June 2003*, ACM Press, New York, 2003.
- [23] M. T. Goodrich, J. S. B. Mitchell, and M. W. Orletsky, Approximate geometric pattern matching under rigid motions, *IEEE Trans. Pattern Anal. Machine Intell.* **21**(4), (1999), pp. 371–379.
- [24] A. Gray, *Tubes*, Addison-Wesley, Reading, MA, 1990.
- [25] M. Gromov, *Metric Structures for Riemannian and Non-Riemannian Spaces*, Progress in Mathematics, Vol. 152, Birkhäuser Boston, Boston, MA, 1999.

- [26] M. Gromov, *Geometric Group Theory*, Vol. 2: *Asymptotic Invariants of Infinite Groups*, (A. Niblo and Martin A. Roller, eds.) London Math. Soc. Lecture Note Ser., Vol. 182, Cambridge University Press, Cambridge, 1993.
- [27] M. Gross et al., *Point Based Computer Graphics*, EUROGRAPHICS Lecture Notes, 2002 (graphics.stanford.edu/~niloy/research/papers/ETH/PointBasedComputerGraphics_Tutorial-Notes.pdf).
- [28] K. Grove, Metric differential geometry, in *Differential Geometry* (Lyngby, 1985), Lecture Notes in Mathematics, Vol. 1263, Springer-Verlag, Berlin, 1987, pp. 171–227.
- [29] A. Ben Hamza and Hamid Krim, *Geodesic Object Representation and Recognition*, Lecture Notes in Computer Science, Vol. 2886, pp. 378–387, Springer-Verlag, Berlin, 2003.
- [30] D. P. Huttenlocher, G. A. Klanderman, and W. J. Rucklidge, Comparing images using the Hausdorff distance, *IEEE Trans. Pattern Anal. Machine Intell.* **15**(9), (1993).
- [31] <http://isomap.stanford.edu>.
- [32] P. W. Jones, Rectifiable sets and the traveling salesman problem, *Invent. Math.* **102** (1990), 1–15.
- [33] D. W. Kahn, *Topology. An Introduction to the Point-Set and Algebraic Areas*, Williams & Wilkins, Baltimore, MD, 1975.
- [34] N. J. Kalton and M. I. Ostrovskii, Distances between Banach spaces, *Forum Math.* **11**(1) (1999), 17–48.
- [35] R. Kimmel and J. A. Sethian, Computing geodesic paths on manifolds, *Proc. Nat. Acad. Sci.* **95**(15) (1998), 8431–8435.
- [36] G. Leibon and D. Letscher, Delaunay triangulations and Voronoi diagrams for Riemannian manifolds, *Computational Geometry 2000, Hong Kong*, ACM Press, New York, 2000.
- [37] G. Lerman, Quantifying curvelike structures of measures by using L_2 Jones quantities, *Comm. Pure Appl. Math.*, **56**(9) (2003), 1294–1365.
- [38] G. Lerman, J. McQuown, A. Blais, B. D. Dynlacht, and B. Mishra, Multiscale strip constructions and their application to gene expression and ChIP-on-chip data, Submitted.
- [39] L. Linsen, Point cloud representation, CS Technical Report, University of Karlsruhe, 2001.
- [40] L. Linsen and H. Prautzsch, Local versus global triangulations, *EUROGRAPHICS '01, Manchester, UK*, The Eurographics Association, 2001.
- [41] C. T. McMullen Lipschitz maps and nets in Euclidean space, *Geom. Funct. Anal.* **8** (1998), 304–314.
- [42] F. Mémoi and G. Sapiro, Distance functions and geodesics on point clouds, Technical Report 1902, IMA, University of Minnesota, Minneapolis, USA, 2003, to appear in *SIAM J. Appl. Math.*, <http://www.ima.umn.edu/preprints/dec2002/1902.pdf>
- [43] N. J. Mitra and A. Nguyen, Estimating surface normals in noisy point cloud data, *ACM Symposium on Computational Geometry*, San Diego, June 2003.
- [44] C. Moenning and N. A. Dodgson, Fast marching farthest point sampling for implicit surfaces and point clouds, Computer Laboratory Technical Report 565, available online at <http://www.cl.cam.ac.uk/users/cm230/docs/pdfs/FastFPSISPC.pdf>.
- [45] A. Desoulhès, L. Moisan, and J. M. Morel, unpublished lecture notes, www.cmla.ens-cachan.fr/Utilisateurs/morel/lecturenote.pdf.
- [46] E. W. Weisstein, Hypersphere point picking, from MathWorld—A Wolfram Web Resource, <http://mathworld.wolfram.com/HyperspherePointPicking.html>
- [47] V. V. Nekrashevych, On equivalence of nets in hyperbolic spaces, *Dopov. Nats. Akad. Nauk Ukr. Mat. Prirodozn. Tekh. Nauki*, (1997), 18–21.
- [48] M. Pauly and M. Gross, Spectral processing of point-sampled geometry, *ACM SIGGRAPH*, ACM Press, New York, 2001, pp. 379–386.
- [49] M. Pauly, M. Gross, and L. Kobbelt, Efficient simplification of point-sampled surfaces, *IEEE Visualization 2002, Boston, MA*, IEEE Computer Society, Washington DC, 2002.
- [50] P. Petersen, *Riemannian Geometry*, Springer-Verlag, New York, 1998.
- [51] P. Petersen, Gromov–Hausdorff convergence of metric spaces, *Differential Geometry: Riemannian Geometry* (Los Angeles, CA, 1990), pp. 489–504, *Proc. Sympos. Pure Math.*, Vol. 54, Part 3, American Mathematical Society, Providence, RI, 1993.

- [52] S. Rusinkiewicz and M. Levoy, QSplat: A multiresolution point rendering system for large meshes, *Computer Graphics (SIGGRAPH 2000 Proceedings)*, New Orleans, LA, ACM Press/Addison-Wesley Publishing Co., New York, 2000.
- [53] K. T. Sturm, Generalized Ricci curvature bounds and convergence of metric measure spaces, to appear in *C. R. Acad. Sci. Paris, Ser. I* (2004), also available at <http://www-wt.iam.uni-bonn.de/sturm/publikationen/paper48.pdf>
- [54] J. B. Tenenbaum, V. de Silva, and J. C. Langford, A global geometric framework for nonlinear dimensionality reduction, *Science* (2000), 2319–2323.
- [55] D. Toledo, Book Review: “Geometric group theory, Vol. 2: Asymptotic invariants of infinite groups”, by M. Gromov, *Bull. Amer. Math. Soc.* **33** (1996), 395–398.
- [56] H. Von Schelling, Coupon collecting for unequal probabilities, *Amer. Math. Monthly* **61** (1954), 306–311.
- [57] M. Zwicker, M. Pauly, O. Knoll, and M. Gross, PointShop 3D: An interactive system for point-based surface editing, *SIGGRAPH*, 2002.